Synaptotagmin is an environmentally sensitive calcium ion sensor

A THESIS

SUBMITTED TO THE FACULTY OF THE GRADUATE SCHOOL

OF THE UNIVERSITY OF MINNESOTA

BY

Jesse Ray Murphy

IN PARTIAL FULFILLMENT OF THE REQUIREMENTS

FOR THE DEGREE OF

MASTER OF SCIENCE

Prof. Anne Hinderliter, Advisor

September 2010

ACKNOWLEDGEMENTS

There were several other people who were instrumental in the success of my research. I would like to thank Dr. Anne Hinderliter for all the guidance and the opportunity to do this work. Without all the help from Jacob Gauer and Kristofer Knutson this project would not have been possible. I would also like to thank students Sarah Kempka, Zach Nelson, and Ryan Sisk for their help. And finally I would like to thank my wife Brianna, who despite a complete lack of interest in science has given me unending support.

ABSTRACT

Exocytosis of neurotransmitters into the presynaptic space is triggered by an influx of Ca^{2+}. Synaptotagmin 1 (Syt1) mediates the fusion of the vesicular bilayer with the presynaptic bilayer through its interactions with Ca^{2+}, phospholipid, and the fusion machinery. The exact mechanism for this information transduction, however, is not well understood. Syt1 contains two homologous binding domains, C2A and C2B, which are tethered to a neurotransmitter containing vesicle by a flexible linker region. We hypothesize that the entire Syt1 C2A domain (linker + C2A) is necessary to translate this binding information into a fusion response. To understand the cooperativity of binding in Syt1 C2A, we studied two commonly utilized C2A constructs. The short construct is simply the structural C2A domain (amino acids 140-265). The second construct possesses more of the flexible linker (amino acids 96-265). To thermodynamically compare the binding behavior between the two constructs, we studied the Ca^{2+} and phospholipid binding using steady state fluorescence and Ca^{2+} binding using ITC. The results were modeled by binding partition functions. The data are consistent with diminished linkage among the binding sites in the short construct. We conclude that the flexible linker domain serves more of an important biological function than tethering the C2 domains to the membrane.

TABLE OF CONTENTS

ABBREVIATIONS

BME	Beta-Mercaptoethanol
Ca^{2+}	Calcium Ion
$CaCl_2$	Calcium Chloride
FRET	Fluorescence Resonance Energy Transfer
IPTG	Isopropyl β-D-1-thiogalactopyranoside
ITC	Isothermal Titration Calorimetry
LUV	Large Unilamellar Vesicle
$MgCl_2$	Magnesium Chloride
mM	Millimolar
MOPS	3-(N-morpholino)propanesulfonic acid
PMSF	Phenyl methyl sulfonyl fluoride
POPC	1-palmitoyl-2-oleoyl-*sn*-glycero-3-phosphocholine (16:0,18:1PC)
POPS	1-palmitoyl-2-oleoyl-*sn*-glycero-3-phospho-L-serine (16:0,18:1 PS)
SDS-PAGE	Sodium Dodecyl Sulfate Polyacrylamide Gel Electrophoresis
Syt1	Synaptotagmin I
$TbCl_3$	Terbium (III) Chloride
μM	Micromolar

LIST OF FIGURES

SCOPE OF THIS THESIS

This thesis presents the characterization of cation and phospholipid binding by Synaptotagmin I C2A domain using thermodynamics as a diagnostic technique. The first chapter is an introduction to Synaptotagmin function and the discrepancy in the literature. The second chapter is a description of protein-lipid and protein-protein interactions and how they are monitored and modeled. The third chapter discusses the synthesis and purification of Synaptotagmin C2A domain. The fourth chapter presents an analysis of cation and phospholipid binding using fluorescence spectroscopy and isothermal titration calorimetry.

CHAPTER 1: SYNAPTOTAGMIN – CA^{2+} AND PHOSPHOLIPID INTERACTIONS

1.0 INTRODUCTION AND BACKGROUND

The modulation and control of regulated exocytosis in most cell types involve proteins known as the synaptotagmins. The human genome possesses approximately 16 identifiable synaptotagmin isoforms; the distribution of these isoforms tends to vary between different cell types (*2*). Their primary function is to act as a fusion-enhancing protein necessary for regulated exocytosis. These proteins act together with the SNAREs to fuse biological membranes, in this case vesicles, with target membranes. The SNARES, or soluble N-ethylmaleimide-sensitive factor attachment protein receptor, form into α-helical bundles and are equally implicated in membrane fusion. Both the synaptotagmins and SNARES are tethered to the membranes with single transmembrane helices, and each has been identified as a critical component in the minimal fusion machinery required for exocytosis (*3-10*). While biochemical techniques can offer clues to the role of synaptotagmin at the presynaptic terminus, they are unable to quantitatively evaluate how information is transduced within the interactions implicated within regulated exocytosis. Therefore, a comprehensive thermodynamic analysis is required to understand the basic mechanisms that trigger fusion through interaction with the membrane.

Synaptotagmin 1 (Syt1) is one of the most studied, yet least understood proteins in the process of regulated exocytosis (*2, 4-5, 11-47*). It is generally accepted to function as the Ca^{2+} sensor in fast release of neurotransmitter into the synaptic cleft (*24, 28, 48-*

50). Syt1 is comprised of an amino terminal transmembrane sequence attached to two cytoplasmic facing C2 domains, C2A and C2B, through a long, flexible linker. The two C2 domains are assumed to localize to the membrane following Ca^{2+} influx. Each C2 domain is composed of an 8-stranded β-sandwich fold with Ca^{2+} binding sites clustered together at the membrane interacting tip of the protein (*19, 51-53*). *In vitro* studies have measured the affinity of C2 domains for Ca^{2+} and membranes and find that binding of Ca^{2+} is more cooperative in the presence of acidic phospholipid compared to binding to Ca^{2+} in solution (*27, 51, 53*).

The function of the C2 domains of Syt1 is to translate binding information into a fusion signal. The C2 domains are the functional binding modules of the synaptotagmins that are known to bind Ca^{2+} as well as phospholipids and numerous other proteins. We hypothesized that rather than implicating specific residues within the C2 domains as being critical to convey binding information, it is the C2 domain in its entirety that is necessary to transmute binding information. A protein or protein module that has conformational flexibility possesses such a theoretical capability (*54*). This suggests that binding and cooperativity, which is a measure of communication between binding sites, will be sensitive to the overall architecture of the protein molecule.

Historically, two different constructs of C2A have been used to study the C2 domains of Syt1 from both a structural standpoint as well as from a ligand binding and biological perspective (*1, 12, 52, 55*). Here, we refer to these two constructs as "short" C2A (KG-C2A [140-265]) and "long" C2A (KG-C2A [96-265]) (Figure 1). The short C2A is basically the isolated C2 domain including the KG cloning tail (*12*). The long

C2A construct possesses an additional 44 residues, amino terminal to the body of the C2 domain (*55*). To aid in the purification process, both proteins were expressed as (*56*), GST-KG-C2A fusions; therefore, both constructs have similar ~17-amino acid N-terminal extension necessary for efficient thrombin cleavage. A thrombin cleavage site exists between the C2 domain and the GST fusion protein. While the differences between the constructs reside distal from the Ca^{2+} binding loops, neither the binding nor the cooperativity in binding toward Ca^{2+} were the same between constructs.

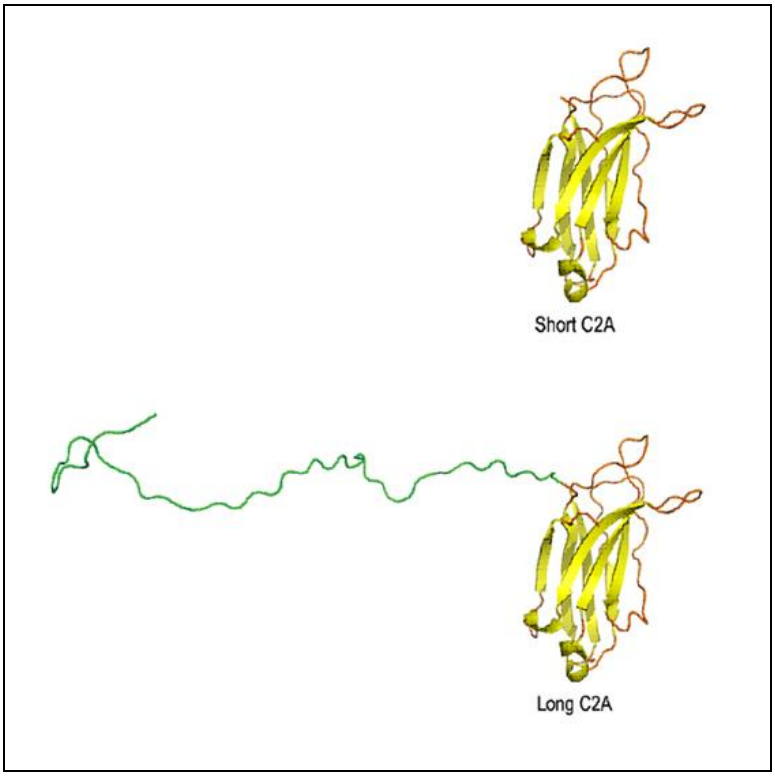

Figure 1

The two commonly used constructs of Syt 1 C2A domain. Shown in yellow are the C2 domains, shown in orange are the binding loops, and shown in green is the additional 44 amino acid segment of the linker region present on the long construct. The C2 domain is the high resolution X-ray structure (PDB ID 1RSY). Modeller program was used to append on the N-terminal residues.

The initial *in vitro* Ca^{2+} and phospholipid binding assays (*12*, *55*) were done using both the short and the long constructs, respectively. Both constructs were shown to bind acidic phospholipid containing vesicles in the presence of Ca^{2+}. A representative C2A construct has not been decided upon. Due to the complexity of Syt 1, the shortened form has been used to identify the minimum protein requirement to bind Ca^{2+} and acidic phospholipids. Both constructs continue to be studied independently. The long construct has been used to determine cation and phospholipid binding affinities using fluorescence spectroscopy and isothermal titration calorimetry (55, 56). Both studies show that the cation binding by the long construct cannot be described by an independent binding model. Furthermore, the fluorescence spectroscopy cation binding data was best fit with a high degree of cooperativity. The long construct has also been used in membrane penetration studies using EPR (51) as well as a number of *in vivo* studies (57-*58*). The short construct has been used for cation and phospholipid binding studies using NMR and fluorescence spectroscopy (*19*). The cation binding elucidated by NMR has been shown to lack cooperativity between cation binding sites. The crystal structure for the short construct has also been solved (*13*).

The assumption in these experiments is that the length of the N-terminal linker is not relevant to the physiological function of the C2 domain, so there have been no controls to justify the use of either C2A domain construct from either a biophysical or biological point of view. This system of the short and long constructs is a means to examine the hypothesis that the overall C2A domain is intimately linked together to disseminate binding information throughout this binding motif.

To test this hypothesis, the binding behavior of these differing constructs of the first C2 domain of Syt1, C2A, was examined. Previously, our group elucidated that the long C2A construct had cation binding behavior consistent with an allosteric transition, or 2-state model (*1*). This model described a weak linkage relationship between the two cation binding sites in the absence of acidic (phosphatidylserine) phospholipid. The presence of acidic phospholipid induces the formation of a third site that binds cation with a greater affinity than the neighboring two cation sites. It is the switching between two states, upon lipid binding, in this case from low affinity to high cation binding affinity, which is the basis for defining this as an allosteric transition. This model also suggests conformational flexibility in the construct. Such flexibility is consistent with a protein that can communicate binding information well away from the binding site (*54*). To quantitate the differences between the long and short constructs, a binding partition function approach was used. This allows the affinity and probability of each binding site of both constructs to be calculated. The constructs diverge in a region well away from their most commonly studied binding sites, Ca^{2+} and phospholipid. We find that the C2A domain of Syt1 exhibits differences in both binding affinity and in cooperativity toward cation and phospholipid. Therefore, the loss of communication between the cation binding sites as evidenced by the loss of cooperativity in the shortened construct is consistent with the C2 domain as a module whose function is to transmit binding information.

CHAPTER 2: PROTEIN-LIPID INTERACTIONS: ROLE OF MEMBRANE PLASTICITY AND LIPID SPECIFICITY ON PERIPHERAL PROTEIN INTERACTIONS

2.0 INTRODUCTION

The cellular membrane is non-uniform in its distribution of proteins and lipids (59-64). There is an intense interest in the basis for the heterogeneous distribution of these signaling components at the membrane. A myriad of names such as rafts, complexes, domains, and lipid shells has been proposed in attempt to capture the fleeting organization of these membrane localized components (65-70). In comparison, older and ongoing bodies of work have established a strong understanding, both experimental and theoretical, of the no ideal mixing behavior of lipids (71-83). These findings have long suggested that both the small, cooperative interactions between lipids as well as the dramatic changes in lipid domain size, as lipid mixtures approach a phase transition boundary provide the organizational underpinning to signal complexes (84). Clustering of signaling components, such as in a lipid domain is a means to enhance the probability of the components interacting (85, 86), and these interactions are necessary to convey a triggered signal in the cell. In an analogous manner, signaling components sequestered into separate regions of the membrane would decrease the probability of interactions occurring (87). Signal transduction complexes are comprised of lipids and proteins where individually the interactions are often small and cooperative so coalescence of the components into a signaling complex becomes very sensitive to the composition of the complex. Furthermore, proteins can redistribute lipids, leading to clustering of lipids and

proteins alike. This is dependent on whether proteins are selective in the lipids they interact with and whether their interactions are of sufficient magnitude to overcome the entropy of mixing. Here, we present a thermodynamic perspective on how the inherent non-random nature of lipid distributions influences the interaction of protein with the membrane surface and how protein-protein interactions can be more probable at the membrane surface than in solution.

2.1 DEFINING PROTEIN-LIPID INTERACTIONS

Proteins and lipids have plasticity in their interactions because the surface of the membrane can be altered by such interactions. When a protein partitions onto the membrane surface, the initial distribution of lipids underneath the protein can differ from the final distribution upon reaching equilibrium. To quantitatively define the system, association constants may be measured between proteins and lipids. This does not, however, convey the sensitivity of such interactions to lipid phase behavior and how this coupling leads to lipid and protein redistribution. To understand the system, the dynamic behavior of the interactions must be conceptualized as the system approaches equilibrium. While the cell does not exist in a state of equilibrium, as this would correspond to death, evaluation of a system at equilibrium does allow the tendencies of the interactions to be ascertained.

The terms binding and partitioning are not used interchangeably as elements of both are needed to convey this model of protein-lipid interactions with lipid selectivity. Binding requires specificity, implies identifiable binding sites and is more robust than

partitioning. Lipid binding sites with both specificity and high affinity have been identified. For example, human prothrombinase complex requires the acidic phospholipid phosphatidylserine (PS) but not a membrane surface to activate the complex (88) and high affinity binding sites for PS have been identified within complex (88).

Partitioning is the non-specific interaction of a protein with the membrane and as it is non-specific (89), the interactions are weak relative to binding. For example, the interaction energy of a charged amino acid (such as lysine) within a peptide with an oppositely charged individual lipid (such as phosphotidylserine) is ~1.4 kcal/mol (90).

2.2 SELECTIVE PARTITIONING AND LIPID ACTIVITIES

We will define a protein-lipid interaction that resides between partitioning and binding as selective partitioning. Rather than using the criteria of an identifiable binding site within the protein for a particular lipid for specificity, selectivity is instead based upon relative affinity within the protein for each lipid in the membrane. If this relative selectivity is large enough, the process by which proteins partitioning onto and off of the membrane surface is not a passive phenomena; it has the capacity to redistribute the underlying lipids.

The initial association of a protein with a membrane surface we described as partitioning, and the extent by which the protein partitions from solution onto the membrane is dictated by lipid chemical activities. The chemical activity of each lipid species in a mixture is determined by the mixing behavior of that lipid, and it is this activity that dictates the strength of association. Each lipid's activity is its effective

concentration, as it can be greater or less than the physical concentration of that lipid within the mixture. Activities of lipids vary with their distribution as described by $a=(c)(\gamma)$ where a is activity, c is concentration of the lipid within the membrane suspension, and γ is the activity coefficient. An activity coefficient is the measure of the deviation of a mixture from a random distribution of components. An activity coefficient greater than one leads to a greater effective than physical concentration; less than one the inverse holds and if the activity coefficient is one, the effective and physical concentrations are equal. Defining the strength of a specific lipid-protein interaction must then be placed within the context of the overall lipid mixture and the effective concentration of the lipids.

Lipid mixtures are inherently non uniform as each lipid species differs slightly in its chemical structure (91). As the differences in lipid chemical structure are small, the unlike nearest neighbor interaction Gibbs free energy, or interaction, energy between like and unlike lipids are also small. Each lipid is surrounded by six nearest neighbors and how weakly attractive or weakly repulsive to one another these lipids are defined by the interaction energy, ω (92). An interaction energy is a measure of, like an activity coefficient, the deviation of the mixture from a random distribution of components in a lattice such as in a membrane. From the partitioning or macroscopic framework, lipids do not act individually, but a microscopic view must also be incorporated to gain understanding of protein influence on lipid reorganization. Interaction energies extend to those lipids underneath the protein as well as the leading edge of lipids beyond the edge of the proteins due to the nearest neighbor nature of lipids.

Upon initiation of a favorable protein-lipid contact, additional protein-lipid and lipid-lipid interactions may be established. Favorable lipid contacts that lie beyond the edge of the protein can be switched underneath the protein resulting in the expulsion of an unfavorable lipid and the gain of a protein-lipid interaction and a favorable nearest neighbor lipid contact. The magnitude of the unlike nearest neighbor interaction energy is indicative of the nearness of the lipid mixture to being separated into phases of distinct lipid composition. As these interaction energies are weakly cooperative and therefore not additive, even small changes in these energies lead to dramatic changes in the distribution of lipids. For a binary mixture of lipids, interaction energies approaching 320cal/mol are nearly phase separated into clusters enriched in each lipid. A positive ω indicates a repulsive interaction between unlike lipids, subsequently; like lipids have a greater tendency to be segregated together. Each lipid in such a scenario has a greater probability to have a like nearest neighbor beyond the edge of an associated protein. As ω decreases, the lipids appear as a nearly random pattern (Figure 2). In a binding framework, especially if lipids are systematically substituted in a mixture to establish a trend, but, the binding behavior is not known, indeed, a change in binding affinity will be observed. This change in affinity may be attributed to an increase in the effective concentration of the lipid with clustering of the preferred lipids and perhaps not to a change in either specificity of the protein for the lipid or presence of a specific lipid binding site. Conversely, a protein could conceivably have a distribution of contact points across its membrane binding surface that favors interacting with an ordered array of unlike lipids. Such a pattern correlates with a negative interaction energy as unlike lipid contacts are

now favored. The mixing behaviors of the lipid mixture can dramatically impact the strength of the interaction of a protein with a membrane surface.

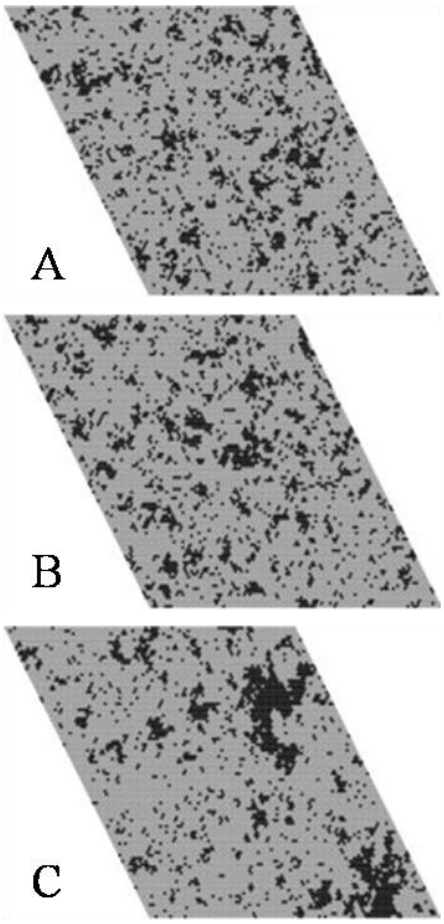

Figure 2.

Monte Carlo simulations of 20% lipids (black dots) in a background of 80% (grey dots) where the interaction energies (ω) increased from 240cal/mol, 280cal/mol to 320cal/mol. This range of interaction energies correlate, for example, to mixtures of the acidic phospholipid 16:0,18:1PS in a background of PCs. Observed is the composition of the lipid mixture can concentrate or disperse the PS. This behavior is consistent within a partitioning framework but could lead to erroneous conclusions if a binding framework that assumes ideal mixing of the ligands is assumed. This is as the interaction of the protein with the membrane surface would be improved by the clustering of like lipids. We would like to thank Professor Paulo Almeida for providing the Monte Carlo simulations.

2.3 PROTEIN-PROTEIN INTERACTIONS AT THE MEMBRANE SURFACE

The membrane is more than a surface which provides a plasticity to potentially be optimized by the interacting proteins; it is a surface which may enhance protein-protein interactions. To illustrate this concept, we will define a scenario in which there is monomeric protein and dimeric protein. Each form of the protein can interact with lipids. If the dimeric and oligomerized form of the protein had greater affinity for lipids, or binds more lipids, than the monomeric form, the dimer would be depleted from solution as it binds lipids. To repopulate the dimer and reestablish equilibrium, the monomer would dimerize. As the dimer has a greater affinity for lipid than the monomer, the overall equilibrium will shift and the other states are depleted with the membrane-bound dimer predominating.

2.4.0 MEASURING PROTEIN-LIPID INTERACTIONS

Although a variety of techniques are used to measure the affinity of a protein for a membrane surface, we will limit our methods discourse to the uses of fluorescence spectroscopy and isothermal titration calorimetry.

2.4.1 FLUORESCENCE SPECTROSCOPY.

Fluorescence spectroscopy is a commonly used technique to detect an interaction between a protein and ligand. Either the ligand or the protein may be the source of the signal. If there is a change of fluorescence signal upon a binding event, this change may be transformed via the Lever Rule into fractional saturation of the macromolecule as a

function of ligand concentration. To interpret the association event, the relationship of saturation of macromolecule to ligand concentration must be related to the equilibration constant.

2.4.2 THE GENERAL USE OF A SIGNAL: LEVER RULE DERIVATION.

$S = f_b*S_b + f_f*S_f$ where $f_b + f_f = 1$ and S is any signal comprised of f_f is fraction free ligand with the corresponding associated signal of S_f and f_b is fraction bound with the corresponding associated signal of $S_{b,}$ with rearrangement $f_b = S\text{-}S_f/S_b\text{-}S_f$ and $f_f = S\text{-}S_b/S_f - S_{b.}$ Therefore, when a system exhibits a change of signal upon an interaction (binding event) as a function of ligand concentration, this change in signal can be plotted as fraction bound versus free ligand concentration. A relationship that relates these variables to an association constant must now be derived to allow evaluation of the interaction in the context of the proposed models. The interaction [P] + [L] = [PL] at equilibrium is represented by K = [PL]/[P][L]. The protein, or any macromolecule, in this scenario exists in two forms, bound ([PL]) and free ([P]). The fraction of the protein in the bound state, f_b, is then equal to [PL]/([P] + [PL]) where ([P] + [PL]) is the distribution of states the protein can exist in the system. In its present state, this equation is not of use. However, by recognizing that with rearrangement, K[L] = [PL]/[P], the equation may be modified. Each form of the macromolecule is normalized against the unbound protein ([P]) by multiplying through by 1/[P]. The fractional saturation (f_b) of the protein is now equal to K[L]/(1 + K[L]) and is a function of an equilibrium constant and the free ligand. When compared to $f_b = S\text{-}S_f/S_b\text{-}S_f$, the connection is apparent, this is the change of signal

with each addition of ligand as well as the dependent variable of the overall binding isotherm, $f_b = K[L]/(1 + K[L])$. The independent variable [L] when representing unbound lipids and more specifically lipids within single lamellar liposomes must be transformed to calculate the change in concentration with interaction with protein. Within a thermodynamic system, the ligand must be accessible to the macromolecule to interact. Therefore, for a protein that interacts with the surface of a liposome, only the outer monolayer is considered. Furthermore, each protein has a greater footprint than an individual lipid, so the number of lipids bound/protein must be determined. This can be problematic if the orientation of the protein on the membrane is not known, but a reasonable estimate can be made. Five to ten lipids could be estimated to be occupied by each protein. If the available lipid concentration is not corrected, the affinity will be underestimated. In this context, correcting multilamellar liposome (MLV) systems is difficult as only a fraction of the lipid comprises the outer layer and small unilamellar vesicles (SUV) have approximately 60% of their lipids on the outer surface. It is important to note that concentrations are used and not a count of individual lipids. Chemical potential (or normalized free energy) of the ligand is directly proportional to the logarithm of its chemical activity. Here, chemical activity is represented for systems that are a dilute aqueous solution as a concentration. A liposome, comprised of individual lipids, is a colloid of a solid phase suspended in a liquid phase and is a homogeneous suspension.

Finally, the independent variable is free lipid, [L]. To calculate free lipid, the previously determined fraction bound (f_b) term that was generated from the change in

signal must be used. For each protein bound to lipid (or to any ligand), there are some number of ligands per protein, this number of ligands multiplied by fraction bound of protein with each addition of ligand is the number of bound ligands. By subtracting the bound ligand from the total ligand at each step of the titration, the free ligand is determined.

2.4.3 EXTENSION BEYOND FLUORESCENCE SPECTROSCOPY

Transformation of a signal is the same regardless of the source of the signal. A few caveats exist, such as the signal in question must have a linear response (93). We most often use fluorescence steady state intensities at a constant wavelength. The system must also be in equilibrium and hence, reversible necessitating that there is not a vast excess of both macromolecule and ligand. A benefit of the use of fluorescence spectroscopy is the relative limited amount of macromolecule necessary to generate signal. This is worth considering when the association reaction involves membrane suspensions. Membrane suspensions strongly scatter light. This can impede the use of optical techniques over a broad range of membrane concentrations.

2.4.4 ISOTHERMAL TITRATION CALORIMETRY

Isothermal Titration Calorimetry (ITC) is another commonly used technique to detect an interaction between protein and ligand. The use of isothermal titration calorimetry to characterize protein-lipid interactions requires orders of magnitude more material (μM) in contrast to fluorescence spectroscopy (nM). The signal in isothermal titration calorimetry is heat and the source of this signal may not be as readily apparent as

with fluorescence spectroscopy. Buffer and pH mismatch between syringe and cell can be a robust source of heat (94). Protein-membrane interactions can be weak (95). This necessitates the use of enough macromolecule for a detectable signal and makes characterizing these interactions more susceptible to the contribution of unanticipated heats.

2.5.0 MODELING OF PROTEIN-LIPID INTERACTIONS

2.5.1 BINDING PARTITION FUNCTIONS

An example of a binding partition function is where the interaction of P + L = PL is represented by the binding isotherm of $f_b = K[L]/(1 + K[L])$. A binding partition function is the distribution of states that the macromolecule exists in and the relative probability of the macromolecule within each state (96, 97). We will illustrate this by examining the normalized probability of the total distribution of states which is commonly represented by a capital Q where Q = [PL] + [P], the denominator of the fractional saturation relationship for f_b. To convert this relationship to a relative probability, Q is divided through by a reference state which is arbitrary in choice but often the free macromolecule is selected. The two states are now [P]/[P] = 1 and [PL]/[P] = K[L], we can now compare the probability of being bound (interacting) to the normalized reference free state (not bound) of one. The normalized probability [PL]/[P] of being bound scales with affinity of macromolecule for ligand (the association constant, K) and with the concentration of ligand, [L] (as expected by Le Chatelier's Principle). When the overall fractional saturation relationship, $f_b = [PL]/([P] + [PL])$ is normalized

by the reference state [P] and the same substitutions are used; the binding isotherm, f_b = K[L]/(1 + K[L]) results.

2.5.2 INTERPRETATION OF BINDING PARTITION FUNCTIONS

The binding isotherm, f_b = K[L]/(1 + K[L]) is an independent site model as being bound is independent of being free. If multiple sites existed of the same (or within 10-fold similarity) affinity, the probability of any one site on the macromolecule interacting with ligand is independent of the other sites. The liposome surface is comprised of lipids that during the course of reaching equilibrium may redistribute, but, as a suspension of liposomes is titrated in as the ligand form, binding of protein to each liposome remains independent of binding to another protein to a separate liposome. The functional form of this isotherm is hyperbolic and all such variations on an independent model will likewise be hyperbolic Figure 3.

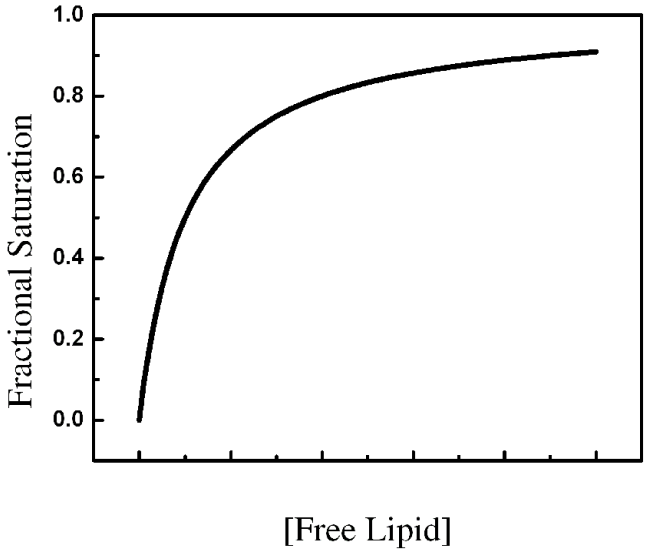

Figure 3. Hyperbolic binding isotherm generated by titrating liposomes into a macromolecule in solution as a ligand. This figure depicts the macromolecule having a liposome binding affinity of $K_L = 2.50x10^{-3}\ \mu M^{-1}$.

2.5.3 COMPARISON TO LANGMUIR MODEL

This may be contrasted to a system where the macromolecule is titrated into a fixed concentration of lipids. This interaction is classically modeled by a Langmuir model. Development of the Langmuir model follows a similar formalism as where liposomes are titrated into a fixed concentration of macromolecule. In the Langmuir model there are as in the previous model, two states but these two states are of the liposome surface which is occupied and unoccupied by the macromolecule. We may represent this fractional saturation of the exposed liposome surface by θ, and the unoccupied surface by $1 - \theta$. The mole fraction of the protein occupied liposome surface (χ_{PL}) is θ and the unoccupied surface is $1 - \theta = \chi_L$ as $\chi_{PL} + \chi_L = 1$. P (Protein in solution) + L (unoccupied surface lipids) = PL (occupied lipids). K_{as} = [PL]/[P][L] may then be rewritten as $K_{as} = \theta/[P](1 - \theta)$ which upon rearrangement yields $\theta = (K_{as})[P]/1 + (K_{as})[P]$. We will focus our discussion on systems where the concentration of lipids varies as these systems are amenable to evaluating the impact of multiple ligands on lipid binding.

2.5.4 BINDING PARTITION FUNCTIONS: LINKED BINDING EQUILIBRIUM

The single site binding model where the liposome is the ligand will be expanded to include an additional ligand, [X] where [X] can be bound by protein independent of the

liposome or where the binding of lipid influences the binding of the other ligand (coupled or linked equilibrium). The benefit of using a binding partition function approach is that the distribution of states of the macromolecule may be directly calculated whether the binding equilibrium is linked or independent. If the binding sites are linked, advantage may be taken of how the binding of one ligand by macromolecule will alter the probability of the macromolecule binding the second ligand. This can allow the determination of the association constant for a ligand, such as to a liposome system that could be difficult to measure directly.

To identify all possible states of the macromolecule that interacts with two ligands; a thermodynamic cycle is constructed. In these scenarios, it will first be assumed that the two ligands interact with the macromolecule independent of one another (Figure 4).

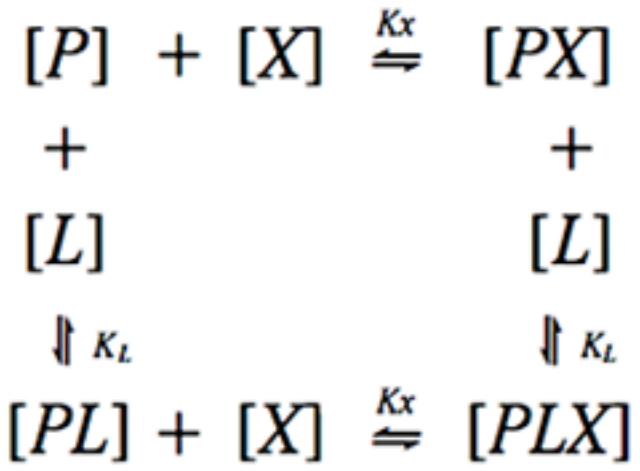

Figure 4. Thermodynamic cycle showing the independent binding relationship the protein [P] has for ligand [X] and liposome [L].

The total distribution of states is then Q = [P] + [PL] + [XP] + [XPL], using the same approach as with a single binding site. After normalizing against the reference state [P], substitutions are made using the association constants for each reaction. The total distribution becomes $Q = 1 + K_L[L] + K_X[X] + K_L[L]K_X[X]$ and the probability of being in the unbound state is 1/Q, of being only bound to liposome is $K_L[L]/Q$, of being only bound to X is $K_X[X]/Q$, and of being doubly bound is $K_L[L]K_X[X]/Q$ Figure 5.

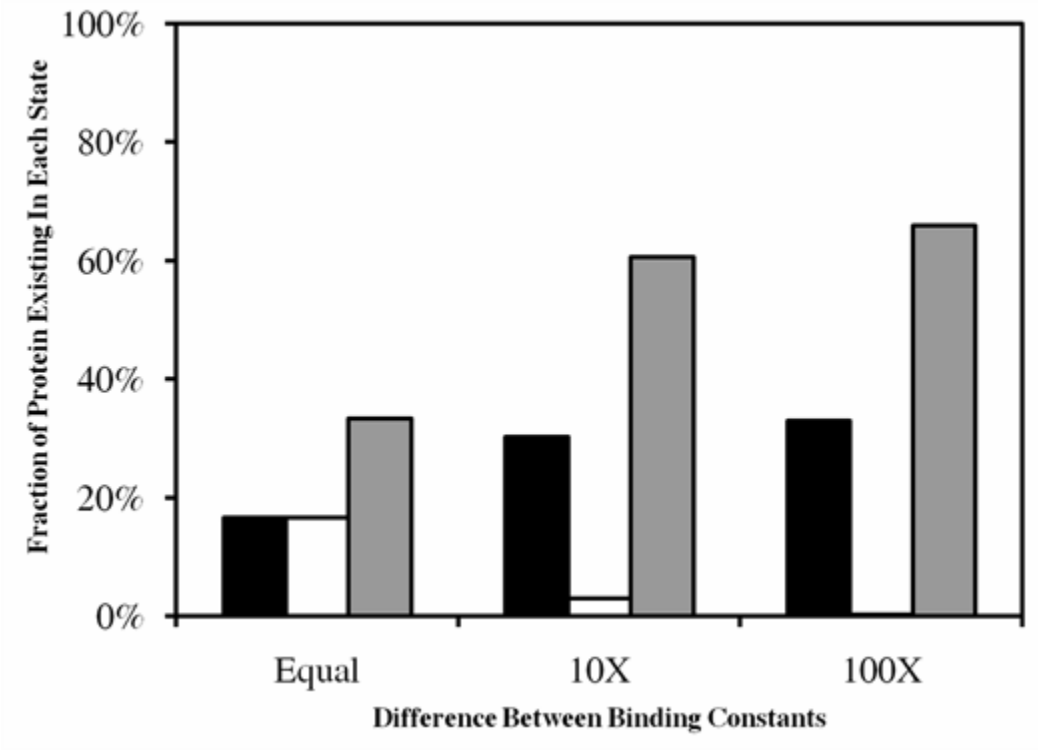

Figure 5. Graphical interpretation of the probability that the protein exists in any of the possible bound states. Here the three possible states are: unbound (shown in black), bound to liposomes alone (shown in white), and bound to ligand [X] alone (shown in gray). We show that when the binding constants the protein has for liposomes and ligand [X] are equal (K_X= 0.05 μM^{-1}, K_L= 0.05 μM^{-1}), there is an equal probability of the protein existing in either state. By changing K_L to 0.05 μM^{-1} and keeping K_X unchanged, the shift in probability towards being bound to ligand [X] alone is clear. A greater difference between binding constants, K_X= 0.05 μM^{-1}, K_L= 0.005 μM^{-1}, has an even more dramatic shift.

$$\theta = \frac{[X]}{Q}\frac{dQ}{d[X]} = \frac{K_X[X]+K_XK_L[X][L]}{1+K_X[X]+K_L[L]+K_XK_L[X][L]} \quad (1)$$

If the binding of one ligand now influences the binding of the second ligand, the distribution of states of the macromolecule, and the consequent probabilities will differ compared to the independent site model. This depends on the extent of the coupling which is reflected in the term σ (Figure 6) and the greater σ, the greater the linkage between the binding sites (Figure 7). This term is incorporated into the thermodynamic cycle (Figure 8) as well as in the calculation of probabilities of each state of the protein. The protein binds ligand [X] in the absence of the liposome with an affinity of K_X. However, the protein if already associated with the liposome now binds ligand [X] with affinity σK_X. The difference in free energies of association are $\Delta G = -RTlnK_X$ compared to $\Delta G = -RTln\sigma K_X$.

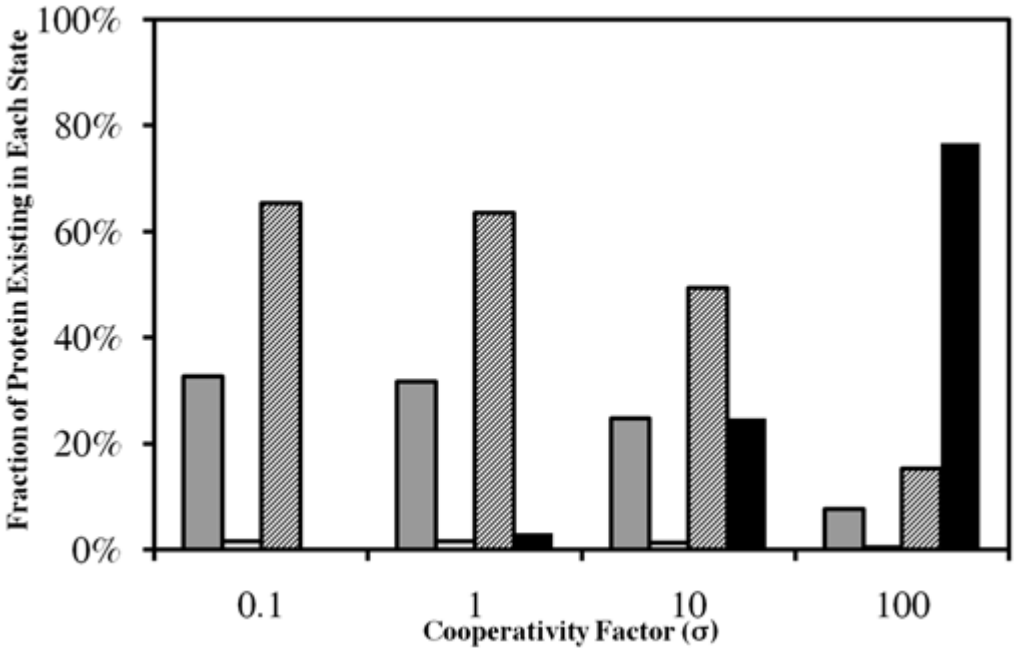

Figure 6. Graphical interpretation of the shift in probability towards doubly bound (bound to both lipid and ligand [X]) by increasing the cooperativity factor σ. Unbound shown in gray, singly bound to lipid shown in white, singly bound to ligand [X] shown in

stripes, and doubly bound shown in black. The plot is based on the following binding polynomial: $Q = 1 + K_X[X] + K_L[L] + \sigma K_X[X]K_L[L]$ where $K_X = 0.05\ \mu M^{-1}$, $KL = 2.50 \times 10^{-3}\ \mu M^{-1}$, [X]= 40.0 μM, and [L]= 20.0 μM. σ was allowed to vary, and the effects are obvious. σ less than 1 indicates negative cooperativity and manifests itself as increasing the probability of being completely unbound. Unit cooperativity is identical to independent binding. Finally, the more positive the cooperativity factor, the higher the probability of being doubly bound.

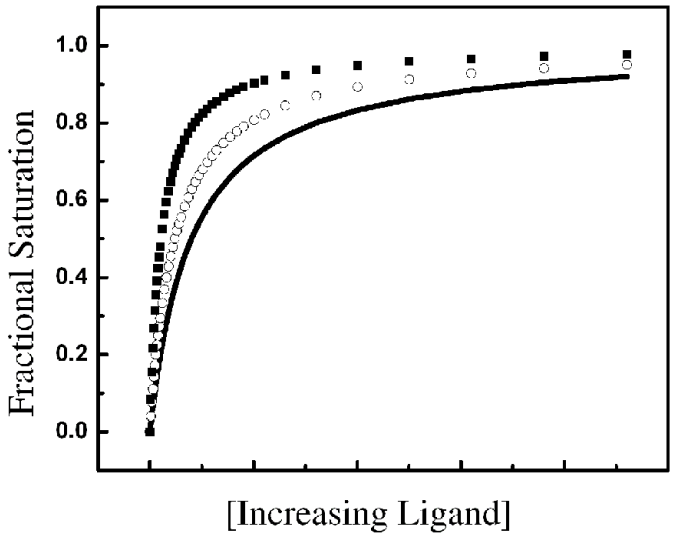

Figure 7. The effects of increasing the cooperativity factor on binding isotherms. The three isotherms were created by plotting equation (2), where K_X was held at 0.05 μM^{-1}, K_L was held at $2.50 \times 10^{-3}\ \mu M^{-1}$ and [L] was held at 20.0 μM. Unit cooperativity (σ=1) is shown in black. A cooperativity factor of 2 is shown in the open circle isotherm and a cooperativity factor of 5 is shown in the black square isotherm. It is clear that an increase in σ increases the affinity, thus becoming fully saturated with ligand at a lower and lower ligand concentration.

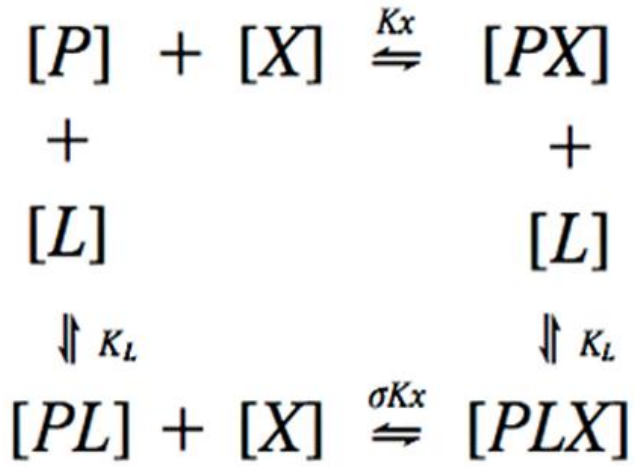

Figure 8. Thermodynamic cycle showing linked binding between ligand [X] and liposome [L].

With linked sites, a change of signal upon binding one ligand [X] may be used to evaluate the binding to liposomes; even if interacting with liposomes does not exhibit a change in signal upon binding. Shown is an example where there is an enhanced affinity for ligand [X] by the protein when the protein is bound to liposome compared to the affinity in the absence of liposome (Figure 9, leftmost panel). Advantage may be taken of this coupling to evaluate the liposome affinity by protein. A suspension of liposomes is titrated into a solution of protein and subsaturating concentrations of [X], binding of liposome increases the affinity of protein for [X] and thereby leading to a change in signal (Figure 8, rightmost panel). A maximum change in signal is achieved upon titrating in liposomes by selecting the concentration of [X] that corresponds to the greatest difference in affinities of protein for ligand [X] in the absence and presence of liposome.

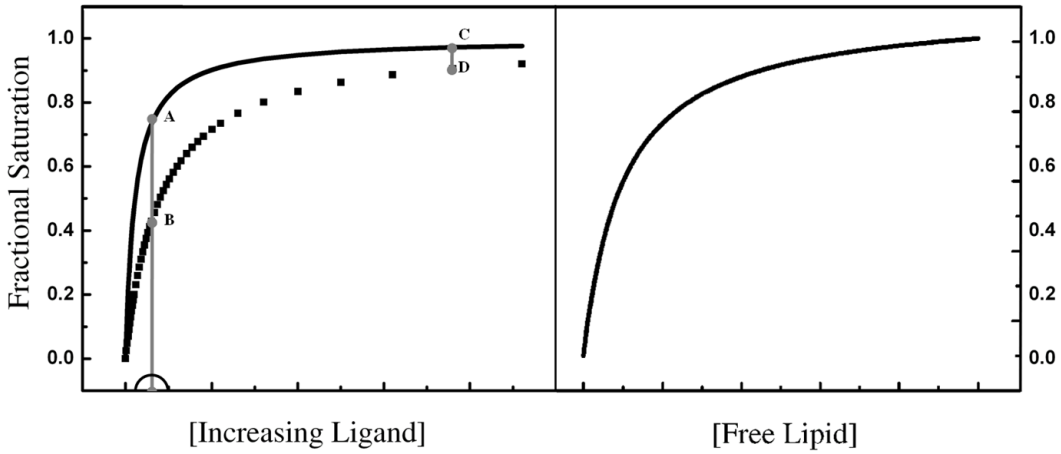

Figure 9

Figure 8 (leftmost panel). Binding isotherms showing the binding of protein to ligand [X] in the absence (dotted line) and presence (solid line) of liposomes. The shift in affinity in the presence of liposomes is indicative of linkage between the two sites. To exploit this linkage relationship for the determination of liposome binding affinity, a lipid titration must be done in the presence of subsaturating ligand [X]. The optimum ligand [X] concentration corresponds to the greatest difference between isotherms (depicted by points A and B, and the ligand [X] concentration is found half circled on the x axis). If a ligand [X] concentration corresponding to a smaller difference between isotherms is used (points C and D), the resulting lipid titration will be greatly truncated as the protein is already much closer to fully saturated with lipid. In this example, using a ligand [X] concentration corresponding to points C and D would lead to approximately 10% of the signal that would have been seen using the ideal concentration.

Figure 8 (rightmost panel). The resulting liposome titration in the presence of subsaturating ligand [X], the concentration of which was determined in Figure 7.

The representative equations for these binding isotherms are:

$$\theta = \frac{[X]}{Q}\frac{dQ}{d[X]} = \frac{K_X[X]+\sigma K_X[X]K_L[L]}{1+K_X[X]+K_L[L]+\sigma K_X[X]K_L[L]} \quad (2)$$

$$\theta = \frac{[L]}{Q}\frac{dQ}{d[L]} = \frac{K_L[L]+\sigma K_X[X]K_L[L]}{1+K_X[X]+K_L[L]+\sigma K_X[X]K_L[L]} \quad (3)$$

It is important to note that for the binding isotherms where one ligand is titrated into the protein suspension and in the presence of a constant concentration of the other ligand, that ligand is also accounted for in the binding isotherm relationship. For the liposomes, once again, only the outer leaflet lipids will be accessible to a peripheral protein.

2.5.5 ISOTHERMAL TITRATION CALORIMETRY TO MEASURE PROTEIN-LIPID INTERACTIONS

When an interaction does not have a representative signal change, the use of linkage relationships is advantageous. A similar approach with isothermal titration calorimetry would complicate interpretation of the signal. The signal for isothermal titration calorimetry is heat. To measure the heats of association of protein for lipid in the presence of a second ligand via the ITC, the second ligand needs to be at saturating levels as attributing the resultant cumulative heats to separate binding processes is difficult (for example see Figure 10, the associated thermodynamic cycle is similar to Figure 8). For instance, subsaturating levels of X would increase the affinity of the protein for lipid, leading to a heat of lipid binding; lipid binding in turn would increase the affinity of protein for X leading to an additional heat as the protein binds X. These heats could be both endothermic, both exothermic or endothermic and exothermic. The binding experiment is much easier to interpret if it reflects a single binding event. Essentially for this approach to be effective, a signal needs to arise from just one of the binding events.

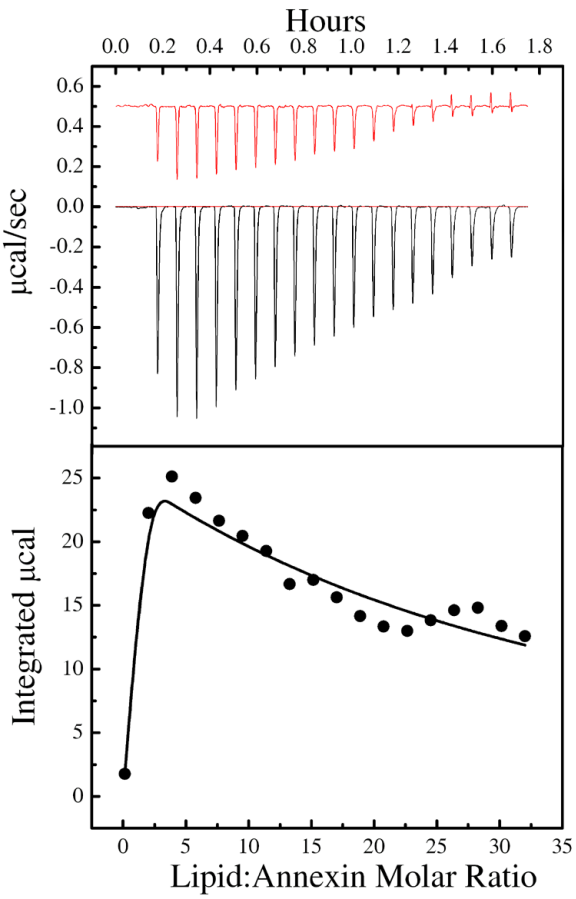

Figure 10.

A representative plot is shown for a protein-lipid interaction where the lipids in the titration are in the gel state to minimize lipid-lipid rearrangement. The conditions were a binary lipid mixture comprised of 14:0,14:0PS:14L0,14:0PC (40%:60%) LUVs in the presence of Ca^{2+} titrated into a solution of 80µM annexin a5 in the presence of the same concentration of Ca^{2+} at 15°C with heat of dilution offset. The lipids in this titration are in the gel state to minimize lipid-lipid rearrangement. The upper panel shows the raw data for the titration with 30mM Large Unilamellar Vesicles (LUVs) in the presence of 0.75mM constant [Ca^{2+}]. The Ca^{2+} concentration present corresponds to 88% saturation of the protein, where the association reaction [PX]+[L] = [PXL] is used to calculate the Ca^{2+} saturation in the absence of lipid with the assumption that each protein binds 9 Ca^{2+} ions independently (98). The lower panel shows the integrated data from the previous raw data following the subtraction of the heat of dilution. The solid line represents the best fit of the data using the independent model and 15mM total outer leaflet lipid concentration as the ligand concentration. The titration was conducted in decalcified 20mM Mops, 100mM KCl pH 7.5. The thermodynamic parameters for this titration are listed in Table

1. Both the Ca^{2+} and lipid titrant solutions were prepared using the dialysate of the protein to maintain a perfectly matched buffer system.

2.5.6 MODELING PROTEIN-PROTEIN INTERACTIONS

Signal transduction complexes are based upon protein-lipid and lipid-lipid interactions, a model for how protein-protein interactions are enhanced at the membrane is presented. Such interactions would lead to further heterogenous distributions of membrane components. A thermodynamic cycle and derivation of the model illustrates how differences in affinities between monomeric and dimeric proteins toward lipid will drive protein interactions at the membrane (Figure 11). [P] is the monomeric form and [PP] is the dimer. If [PP] has greater affinity for a lipid than [P], the addition of this ligand will induce the protein to bind the membrane as a dimer. How cooperatively this occurs will depend on the difference in ligand affinity between the two forms of the protein and the concentration of [P] and [PP].

$$
\begin{array}{ccccc}
[P] & + & [P] & \overset{Kp}{\rightleftharpoons} & [PP] \\
+ & & & & + \\
[L] & & & & [L] \\
\Downarrow K_L & & & & \Downarrow Kp_L \\
[PL] & + & [P] & \overset{K_{LP}}{\rightleftharpoons} & [PPL]
\end{array}
$$

Figure 11.

Thermodynamic cycle showing the dimerization of proteins, [P] and interaction with lipid [L] of the monomers and dimers.

The fraction of protein existing as a dimer is simply all the dimerized states divided by all the possible states (Eq. 4).

$$\theta_{Dimerized} = \frac{[PP]+[PPL]}{[P]+[PP]+[PL]+[PPL]} \quad (4)$$

To obtain a more useful form of this equation, each term must be normalized against a reference state which we select as the monomeric form ([P]). Then, substituting each normalized term with the respective equilibrium constant from the thermodynamic cycle, equation 5 is generated.

$$\theta_{Dimerized} = \frac{K_P[P]+K_P[P]K_{PL}[L]}{1+K_P[P]+K_L[L]+K_P[P]K_{PL}[L]} \quad (5)$$

This equation can be simplified by factoring ($K_P[P]$) from the numerator and rearranging the denominator.

$$\theta_{Dimerized} = \frac{K_P[P](1+K_{PL}[L])}{1+K_L[L]+K_P[P](1+K_{PL}[L])} \quad (6)$$

A similar approach can be used to generate the fraction in the monomeric state.

$$\theta_{Monomer} = \frac{1+K_L[L]}{1+K_L[L]+K_P[P](1+K_{PL}[L])} \quad (7)$$

The ratio of the fraction dimerized to the fraction in the monomeric state may now be calculated, we define this as $K_{Apparent}$.

$$K_{Apparent} = \frac{\theta_{Dimer}}{\theta_{Monomer}} = K_P[P]\frac{(1+K_{PL}[L])}{1+K_L[L]} \quad (8)$$

In this final form, it is obvious that the greater K_{PL} is than K_L, the higher the probability that the protein will exist as a dimer at the membrane. Conversely, if K_L is greater than

K_{PL}, there would be a higher probability of the protein existing as a monomer. It is also important to note that if K_{PL} is greater than K_L then the dimeric form has a higher affinity for lipid than the monomer. This will also further drive the protein into the dimeric form.

We can also introduce a scenario where the dimer and monomeric form can interact with difference numbers of lipids. The representative equation is:

$$K_{Apparent} = \frac{\theta_{Dimer}}{\theta_{Monomer}} = K_p[P]\frac{(1+K_{PL}[L])^n}{(1+K_L[L])^m} \quad (9)$$

If n > m, or the dimer binds more lipid than the monomer, even if $K_{PL} \sim K_L$, the protein will have a greater probability to be a dimer with membrane.

2.6.0 SYNOPSIS

Proteins partition onto the membrane surface from the surrounding solution and this extent of partitioning will vary with lipid composition. How partitioning varies with lipid composition and lipid concentration can be difficult to determine as partitioning and binding is dependent on the chemical activity of the unbound lipid within the mixture. As relatively few lipid mixtures have been characterized on a rigorous thermodynamic level of the almost infinite possible combinations, this becomes a limiting factor. To gain predictability of which lipids that proteins interact with as well as which lipid mixtures proteins can redistribute requires such characterization.

Depending on the strength of the lipid-protein interaction and how specifically a protein interacts with a particular lipid, this interaction can redistribute the lipids within the mixture. It is the coupling of the inherent nonrandom mixing behavior of lipids with protein selectivity in association which leads to lipid reorganization and nonrandom

distributions of proteins on the membrane surface. If the lipid mixture was randomly distributed, or, the protein binds each of the lipids within the mixture with equal affinity, the protein-lipid interaction would not redistribute lipids (99, 100). Defining whether a protein has the capacity to reorder a membrane surface is not necessarily straightforward. To explore how much difference in affinity that is necessary for one lipid over another in a binary lipid mixture by a protein for the protein to redistribute the lipids, a series of Monte Carlo simulations were performed (kindly provided by Paulo Almeida). The system was comprised of a binary lipid mixture of 20%PS in a background of 80%PC (phosphatidylcholine) with a lipid-lipid interaction parameter of 280 cal/mol. There is a base protein-lipid interaction strength of 5 kcal/mol for the membrane comprised of PS and PC and the protein interacts with 19 lipids. To this base protein-lipid interaction, specificity is added with an extra PS-protein interaction. This extra interaction for each PS with protein was increased in increments of 200 from 200 cal/mol to 1000 cal/mol (Figure 11). Observed is with additional interaction energy of 600 cal/mol for each PS contact with the protein, clustering of PS as well as proteins occurs in tandem. In comparison, an extra interaction energy of 200 cal/mol to 400 cal/mol did not lead to a pronounced redistribution of proteins and lipids while an additional interaction energy of 800 cal/mol to 1000 cal/mol lead to an increasing to almost complete segregation of lipid and proteins. The sensitivity of the system to small differences in specificity to which lipid a protein preferentially interacts with is apparent.

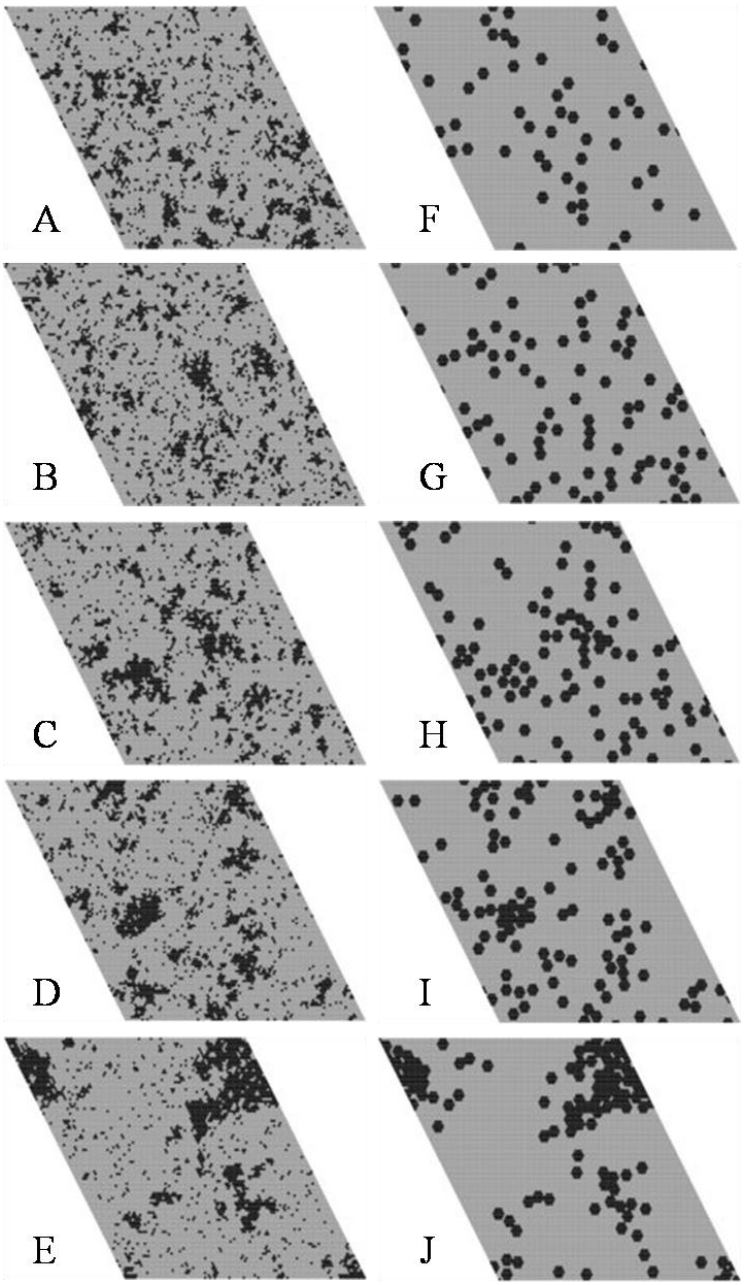

Figure 12

The system was comprised of a binary lipid mixture of 20%PS (black dots) in a background of 80%PC (grey dots) with a unlike nearest neighbor interactions, ω, of 280cal/mol. There is a base protein-lipid interaction strength of 5kcal/mol for either PS or PC and the protein interacts with 19 lipids. To this base protein-lipid interaction, specificity is added to the interaction with an extra PS-protein interaction. This extra interaction for each PS with protein was increased in increments of 200 from 200cal/mol (A), 400cal/mol (B), 600cal/mol (C), 800cal/mol (D) and 1000cal/mol (E). 100 proteins

were added to the system for each simulation (shown as hexagons in rightmost panels), the numbers of proteins associated with the membrane surface increased as extra interaction energy increased where 57 proteins were associated with the surface at 200cal/mol (F), 80 proteins were associated at 400cal/mol (G), 91 proteins were associated at 600cal/mol (H), 97 proteins were associated at 800cal/mol (I) and 100 proteins were associated at 1000cal/mol. If the protein-lipid interaction strength is increased to 8kcal/mol, all of the proteins were bound for each of the extra interaction energies but the protein and lipid simulations appeared the same as with 5kcal/mol. We would like to thank Professor Paulo Almeida for providing the Monte Carlo simulations.

In quantitating protein-lipid interactions, the concept of specificity becomes relevant although specificity must be carefully defined. Specificity in this case, we define as an interaction of a protein for a particular lipid in the mixture over the other lipids present. The question is then raised, how much binding affinity signifies specificity? Specificity is enough affinity that the protein can induce reorganization of the membrane surface upon interaction with the surface. In this sense, the protein is forming not a lipid binding pocket, but the optimal lipid surface to maximize protein-lipid contacts. In other words, the protein forms the lipids into its binding surface. This malleability is a manifestation of the small interaction energies between lipids. If lipids strongly adhered to one another, a protein induced optimization of its membrane binding surface would not be possible. The surface would be static rather than plastic and correspondingly less responsive to protein interactions.

CHAPTER 3: SYNTHESIS OF SYNAPTOTAGMIN I C2A DOMAIN

3.0 SYNTHESIS AND PURIFICATION OF SYNAPTOTAGMIN C2A DOMAIN

The KG-C2A [140-265] plasmid was transformed into BL21-DE3 competent cells and the DNA sequencing was conducted by Northwoods DNA, Inc. Large 1 liter cultures were inoculated with small 5.0 mL cultures (overnight growth). The 1.0 liter cultures were allowed to grow in the presence of 100 μg/mL ampicillin until an optical density of 0.8-1.4 was reached. After induction with 1.0 mM IPTG, the cultures were incubated for an additional 5 hours. The cells were harvested by centrifugation and 20 grams were lysed via sonication in lysis buffer (20 mM MOPS, 100 mM KCl, Complete EDTA-free tablets (Roche), pH 7.5). Following sonication, the cellular debris was separated by centrifugation for 30 minutes at 16,000 rpm. The supernatant containing Syt1 C2A was treated with Benzonuclease (10 units/mL) in the presence of 5.0 mM $MgCl_2$ overnight. The DNA was separated by centrifugation followed by sterile filtering with a 0.4 μm filter. The GST fusion protein was allowed to bind 50.0 mL of equilibrated GST-resin for 2 hours at 4° C. 500 mL of lysis buffer was passed through the column to elute any unbound protein. The A_{280} was monitored throughout via Nanodrop to ensure all contaminating protein was washed from the column. 30 ml of Thrombin (6.0 μg/mL in lysis buffer) was added directly to the column where the media was re-suspended and allowed to rock at room temperture for 5 hours. C2A was eluted from the column with

lysis buffer. The protein solution was aliquoted into 50 ml Falcon tubes where each tube was mixed overnight in the presence of 100 µl p-Aminobenzamidine-Agarose (Sigma) to remove Thrombin. The protein solution was separated from the media by sterile filtering with a 0.4 µm filter and was passed over a clean GST-resin column to ensure separation of any remaining free GST. Following the purification, SDS-PAGE was used to determine purity. Recombinant C2A was dialyzed in the presence of Chelex-100 resin to remove any contaminating Ca^{2+} and concentrated to ~500 µM using Amicon concentrator units with a 10kDa cutoff. Final purity was determined to be >95% by SDS-PAGE densitometry (Figure 13) and concentration was determined using a Nanodrop with an extinction coefficient of 12090 M^{-1}.

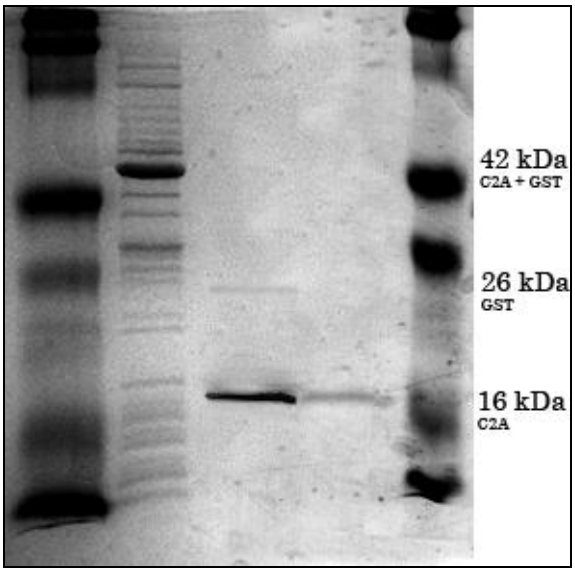

Figure 13

Scheme of Syt 1 C2A purification. From left to right (Molecular Weight Ladder, Cell Lysis, First Affinity Chromatography, Final pure C2A, Molecular Weight Ladder).

CHAPTER 4: SYNAPTOTAGMIN IS AN ENVIRONMENTALLY SENSITIVE CA^{2+} SENSOR

4.0 INTRODUCTION

Synaptotagmins are a family of proteins containing two cytoplasmically facing C2 domains tethered to neurotransmitter containing secretory vesicles with a flexible linker region and short transmembrane sequence. It is widely accepted that these proteins are the Ca^{2+} sensor in fast release exocytosis. Syt 1 has been shown to bind calcium ions and acidic phospholipids to regulate this process. Despite extensive study, the mechanism for this signal transduction is unknown. Two constructs of Synaptotagmin 1 C2A domain ("short" C2A (KG-C2A [140-265]) and "long" C2A (KG-C2A [96-265]) are used interchangebly throughout the literature. The additional 44 amino acids present on the N-terminus of the long construct has been assumed to have no impact on the binding behavior of the protein.

Here, for the first time, we present a direct comparison of the binding characteristics of the short and long constructs. We show that without the linker region, the isolated C2A domain binds Ca^{2+} strictly independently in the absence of lipid and with greatly diminished cooperativity in the presence of lipid. This difference was seen using the partition function analysis outlined in Chapter 2 as well as using ITC. Isothermal titration calorimetry has allowed the direct measure of the difference in enthalpy associated with cation binding by the two constructs under the same conditions.

We show that both the long and short C2A Ca^{2+} binding data sets cannot be described using the same model.

4.1 MATERIALS AND METHODS

Materials. 1-Palmitoyl-2-oleoyl-*sn*-glycero-3-phosphocholine (POPC or 16:0,18:1PC) and 1-palmitoyl-2-oleoyl-*sn*-glycero-3-phosphoserine (POPS or 16:0,18:1PS) were from Avanti Polar Lipids, Inc. (Birmingham, AL). Potassium chloride was puriss-grade and 3-morpholinopropanesulfonic acid (MOPS) was Biochemika grade from Fluka (Sigma Corp.) (St Louis, MO). Chelex-100 ion-exchange resin was from Bio-Rad Labs (Hercules, CA). Chloroform, methanol and benzene were HPLC-grade (J.T. Baker, Mallinckrodt Baker, Inc., Phillipsburg, NJ). All other chemicals were reagent grade**.**

Preparation of Large Unilamellar Vesicles (LUV). Mixtures of PC and PS were prepared by aliquoting lipid stocks in chloroform into borosilicate culture tubes. The chloroform was removed by drying the lipids into a thin film using argon and a vacuum pump at less than 20 mTorr. The samples were then lyophilized from benzene/methanol and hydrated in 20 mM MOPS, 100 mM KCl, pH 7.5. 200 µl of 4 mM multilamellar vesicles (MLV) were extruded through a 0.1 µm pore size polycarbonate filter (Costar Scientific Corp., Cambridge, MA) 30 times using a hand held extruder (AVANTI POLAR LIPIDS, INC., Birmingham, AL).

Fluorescence Spectroscopy. The binding affinity of C2A for Tb^{3+} and lipid was determined by interpreting the fluorescence resonance energy transfer (FRET) from the single tryptophan in C2A to bound Tb^{3+}. The lanthanide, Tb^{3+}, has been shown to be an accurate mimic for Ca^{2+} as it has a similar ionic radius but higher charge density.

Cation binding curves were generated by monitoring the quenching of fluorescence from the single tryptophan and several tyrosine residues in synaptotagmin I C2A. The excitation and emission wavelengths used were 295 nm and 343 nm, respectively. The fluorescence energy transfer from the protein to bound Tb^{3+} resulted in decreasing fluorescence intensity. This loss of signal was normalized via the Lever rule and plotted as fractional saturation. Total ligand added was corrected to bound ligand at each fractional saturation value after accounting for the total number of ligands C2A can bind when fully saturated. Finally the bound ligand was subtracted from the total ligand added at each point, resulting in free ligand. All binding curves were then plotted as fractional saturation versus [free ligand].

To directly measure the lipid binding affinity of C2A, a membrane incorporated probe, Dansyl DHPE (50:40:10 POPC:POPS:Dansyl DHPE) was titrated into a C2A solution in the form of LUVs. This probe can be used as it has the ability to accept fluorescent energy transfer from the tyrosine residues in C2A. The excitation and emission wavelengths used were 283 nm and 344 nm, respectively. The results from this technique were treated in much the same way as the Tb^{3+} titrations. The data were plotted as fractional saturation versus [free lipid], assuming C2A binds 5 lipids. Here [free lipid] is referring to free exterior lipid concentration which is half of the total lipid concentration. This accounts for the fact that the protein has access to only the outer leaflet of the LUVs.

Sample Design and Control Experiments. All titrations were done using a Fluorolog Steady State Fluorimeter with double emission and double excitation monochromators

from Horiba Jobin Yvon interfaced to a Neslab water bath and thermostatted at 20^{o}C, with 0.4-0.5 µM C2A in decalcified 2mM MOPS, 100mM KCl, pH 7.5 buffer. All samples were prepared in a quartz cuvette by use of Hamilton syringes. After each ligand addition, the sample was vortexed and allowed to equilibrate for 10 minutes before scanning. To quantify the contribution of photobleaching to decreasing fluorescence intensity, time trace experiments were done for each experimental condition. Each time trace scan was conducted for 800 seconds, while excitation and emission wavelengths used were the same from each experiment condition. The resulting loss of signal in each experimental condition was 7.3% for 0.4 µM C2A, 12.5% for 0.4 µM C2A with 49.5 µM total Dansylated LUV, and 3.2% for 49.5 µM Dansylated LUV. These results indicate a small photobleaching contribution to total loss in fluorescence intensity. Stock protein concentrations for both constructs were determined using a Nanodrop spectrophotomer with a molar extinction coefficient of 12090 $M^{-1}cm^{-1}$ at 280 nm

Binding Isotherms. Binding isotherms were derived from the binding partition function as described by (*59*). Briefly, the binding partition function contains a term proportional to the probability of observing each state of the protein. To obtain the binding isotherm (θ) from the partition function (Q), the following derivative is calculated (Equation 1).

$$\boldsymbol{\theta} = \frac{[X]}{NQ}\frac{dQ}{d[X]} \qquad (1)$$

Where θ is the fractional saturation of cation binding sites on C2A, or the fraction of proteins bound to lipid. X refers to free (i.e unbound) [Tb^{3+}] , [Ca^{2+}], or [Lipid]. N is the number of ligand binding sites (when X is referring to [Tb^{3+}] or [Ca^{2+}], then N is 2 in the

absence of lipid and 3 in the presence of lipid (12) and when X is referring to [L], then N=1 as the protein binds to a single liposome comprised of lipids), and Q is the partition function which is the distribution of states the protein can be found in the experiment. In solution, the cation binding of C2A can be described by the partition function q_0 (Equation 2).

$$q_0 = 1+2K[X]+K^2[X]^2 \quad (2)$$

Where K is the cation association constant.

A two state transition model can be used to describe the change induced by the presence of lipid. The presence of acidic lipid causes the third cation binding site to become available and can be modeled by the global partition function,

$$Q= q_0+K_L[L]q_1 \quad (3)$$

Where K_L is the lipid binding constant and q_1 is described by (Equation 4).

$$q_1= 1+2K[X]+K^2[X]^2+\sigma K^3[X]^3 \quad (4)$$

The binding isotherm (θ), used to fit the binding plots, can be calculated for cation and lipid binding by differentiating the partition functions with respect to either ligand ([X] or [L]). In the case of lipid binding in the absence of cation, the partition function used is

$$Q_L= 1+K_L[L] \quad (5)$$

Isothermal titration calorimetry (ITC). ITC experiments to determine the binding of Ca^{2+} to Syt1 C2A were performed using a TA Instruments Nano ITC at 18°C. The Ca^{2+} titrant was hydrated in protein dialysate consisting of 20 mM MOPS and 100 mM KCl, pH 7.5 that was passed through Bio-Rad 100 Chelex resin to remove cation impurities

and then filtered using a 0.2 μm sterile filter. The Ca^{2+} stock used in the experiments was verified through the use of BAPTA method (*60*) and a Ca^{2+} electrode (Fisher). In ITC experiments, the cell Syt1 C2A concentration was directly measured using spectrophotometry (Nanodrop) prior to the experiment. The calorimetric sample cell was filled with 1.300 mL of thoroughly degassed solution consisting of 0.543 mM of the short Syt1 C2A construct while the syringe was loaded with 250 μL of 15 mM $CaCl_2$. The stir speed was 250 rpm and the interval between injections was 300 s. Ca^{2+} titrant was added in a 1 μL injection to displace air from the syringe followed by 27 × 9 μL injections. The raw heats were integrated and the heat of dilution subtracted by injecting the Ca^{2+} into buffer without protein. The integrated heats were fit using the independent site binding model.

4.2.0 RESULTS

4.2.1 Cation Binding by Syt1 short C2A, KG-C2A [140-265]

To use binding partition functions, numerous measurements must be made, and the binding conditions must be varied. This enables the binding isotherms to be globally fit by a limited set of parameters. Fluorescence spectroscopy is one such technique utilized to make such measurements, however, the short construct of C2A does not exhibit any endogenous alterations in its intrinsic fluorescence upon binding Ca^{2+} or phospholipid. To circumvent this limitation, the fluorescence mimics of the C2A ligands of Ca^{2+} and phospholipid, Tb^{3+} and Dansyl DHPE, respectively, were employed. Tb^{3+} undergoes luminescence if directly excited or indirectly by fluorescence energy transfer

from tryptophans when ligated by a protein. Tb^{3+} binding is then evident by the loss of intrinsic protein fluorescence as well as the appearance of a primary emission peak at 545 nm and a secondary emission at 490 nm (*61*). As luminescence is a forbidden transition, it is weak relative to the protein fluorescence; therefore, the greater signal arising from the loss of protein fluorescence was used to generate the binding isotherm. In a similar manner, the loss of protein fluorescence is used to quantitate binding of C2A to membrane.

Binding experiments must be designed such that there is free ligand (Ca^{2+} or phospholipid) at every experimental point. This necessitates the presence of a greater concentration of liposome than protein in the system as the protein may only bind the outer leaflet of the membrane. The resultant protein fluorescence that is transferred to Dansyl DHPE is relatively small compared to the background Dansyl DHPE fluorescence. In comparison, the loss of protein fluorescence due to FRET to the Dansyl DHPE is a much greater proportion of the original protein signal. Because of this, the loss of protein fluorescence was used to generate the binding isotherm for both fluorescent ligands, as it was the most sensitive to measure binding to C2A. The resultant binding isotherms were fit allowing only one free variable at a time. The binding affinities obtained from cation and phospholipid titrations (Figures 14 and 15) were used as constants in later titrations (Figure 16). This way the more complicated models (Figure 16) were constrained, allowing only the cooperativity factor (σ) to float.

The binding curve generated from the titration of the short C2A with $TbCl_3$ in the absence of liposome is shown in Figure 14A. Analysis of the hyperbolic binding curve using Equation 2 suggests that C2A binds two cations with equal affinity in the absence of lipid vesicles. Each site binds cation with affinity of $K=5x10^4\ M^{-1}$, corresponding to -6.3 kcal/mol at 20°C. The lack of cooperativity is also suggested by the strongly hyperbolic shape of the binding isotherm. Therefore, there is a clear difference in how the short and long C2A construct bind Ca^{2+} (Figure 14). In a previous study, the long C2A construct has been shown to bind cations in a cooperative manner; the second binding site having 18 times higher affinity than the first site (*1*).

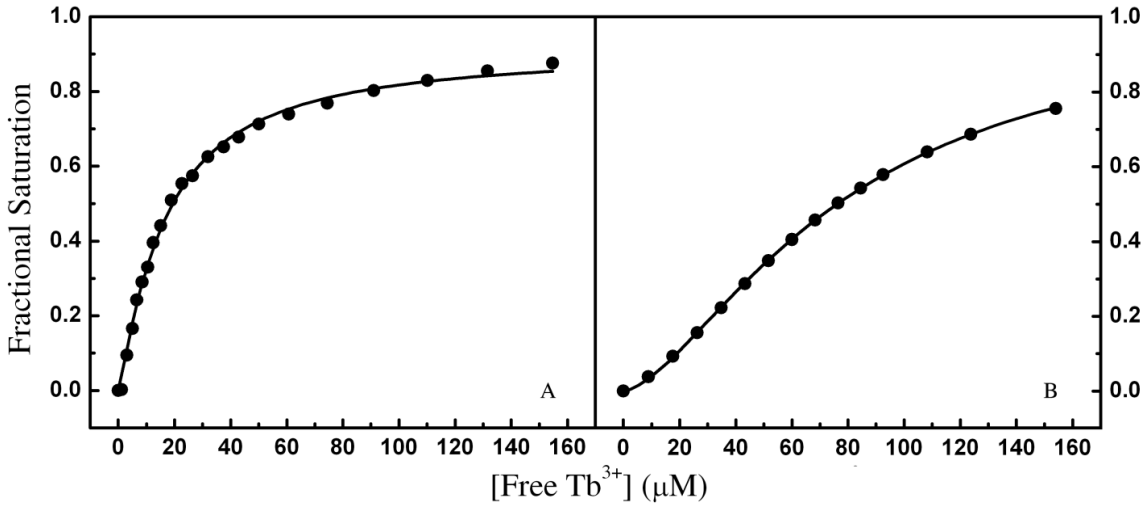

Figure 14

(A) Tb^{3+} binding to 0.4 μM Syt1 C2A short construct (amino acids 140-265) in the absence of lipid. The quenching of tryptophan fluorescence upon Tb^{3+} binding was converted via the Lever rule, into fractional saturation. The total [Tb^{3+}] titrated into solution was corrected for [free Tb^{3+}] assuming C2A binds two cations in the absence of lipid. All titrations were carried out in decalcified 2mM MOPS, 100 mM KCL, pH 7.5. The binding curve was fit using Equation 2. This shows the two cation binding sites have equal affinity of $K= 5x10^4\ M^{-1}$. The difference in the shape of the binding curves of A and B is obvious. The strongly hyperbolic shape is also indicative of independent binding.

(B) Tb^{3+} binding to 0.55 μM Syt1 C2A long construct (amino acids 96-265) in the absence of lipid. Data was plotted as fractional saturation versus [free Tb^{3+}] by the same process as Figure 14A. This data was best fit with an additional cooperativity factor (σ=18) at the second binding site (*1*).

4.2.2 Membrane Binding by Syt1 short C2A

To directly measure the lipid binding affinity (K_L), titrations of C2A with a membrane incorporated probe, Dansyl DHPE (50:40:10, POPC:POPS:Dansyl DHPE), were carried out in the absence and presence of Ca^{2+} (Figure 15 left panel). The titration in the absence of cation was analyzed using Equation 5 and resulted in a lipid binding affinity of $K_L = 3.3x10^5\ M^{-1}$, corresponding to -7.4 kcal/mol at 20°C. To analyze the lipid binding data in the presence of cation, Equation 3 was used. The data was fit by fixing the cation binding affinity $K = 5x10^4\ M^{-1}$ (obtained from analysis of Figure 14A) and the resulting lipid binding affinity was $2.7x10^5\ M^{-1}$, corresponding to -7.3 kcal/mol. The lipid binding affinity changes by a negligible 0.1 kcal/mol upon addition of cation; indicating that the lipid and cation sites bind independently. The same approach has been done with the long construct (Figure 15 right panel) (54). This titration was done using 0.4 μM long C2A in the absence of Ca^{2+} (open circles) and the presence of 2.0 μM Ca^{2+} (black circles). The shift in binding affinity corresponds to an additional 0.5 kcal/mol free energy of lipid binding in the presence of Ca^{2+}.

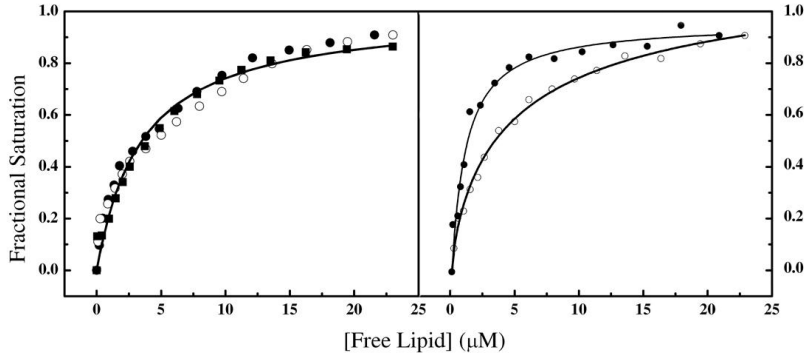

Figure 15

(Left Panel) Titration of short C2A with a membrane incorporated probe Dansyl DHPE (50:40:10 POPC:POPS:Dansyl DHPE). To account for the fact that only the exterior of the liposomes is available for protein binding, the total lipid concentration was halved. The bound lipid was then subtracted from total exterior lipid to obtain the [Free Lipid]. The black squares represent the titration in the absence of Ca^{2+} the black circles represent the titration in the presence of 2 μM Ca^{2+} and the open circles represent the titration in the presence of 40 μM Ca^{2+}. The highly overlapping binding curves show that the binding of lipid is not affected by the presence of cation; further indicating that the lipid binding and cation binding sites are weakly linked, if not independent. The lipid binding affinity, K_L, is $3.3x10^5$ M^{-1} in the absence of Ca^{2+} and $2.7x10^5$ M^{-1} in the presence of both [Ca^{2+}], corresponding to a 0.1 kcal/mol difference at 20°C. The fit line shown here was generated by globally fitting the three data sets using Equation 3.

(Right Panel) Titration of long C2A with membrane incorporated probe Dansyl DHPE (65:25:10 POPC:POPS:Dansyl DHPE). To account for the fact that only the exterior of the liposomes is available for protein binding, the total lipid concentration was halved. The bound lipid was then subtracted from total exterior lipid to obtain the [Free Lipid]. The open circles represent the titration in the absence of Ca^{2+}. The black circles represent the titration in the presence of 2 μM Ca^{2+}. The shift in binding affinity corresponds to an increase of 0.5 kcal/mol in free energy of lipid binding in the presence of Ca^{2+}.

4.2.3 Linkage of Binding Sites of Syt1 short C2A

To quantify the effect that the presence of lipids has on cation binding, Tb^{3+} was titrated into a solution of C2A and 112 μM total 60:40 POPC:POPS. By increasing the lipid, we sought to determine if there was a weak linkage between the cation and lipid

binding sites. This weak linkage is evident by the slight shift toward higher cation binding affinity when lipid is present when this isotherm is overlayed with the cation binding isotherm in the absence of lipid (Figure 16). The lipid presence inducing an increased cation affinity but maintaining a hyperbolic binding isotherm is indicative of weak cooperativity between the sites.

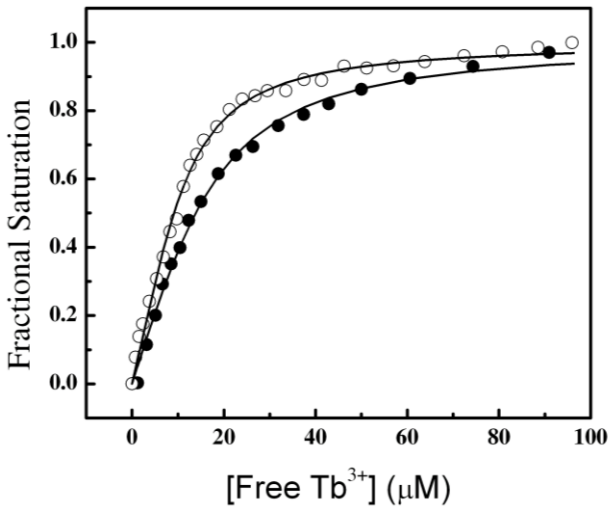

Figure 16

Short C2A Tb^{3+} titration in the presence of 112 μM 60:40 POPC:POPS (open circles). The binding curve was fit using Equation 4, holding $K = 5.0x10^4\ M^{-1}$, $K_L = 3.3x10^5\ M^{-1}$, [P] = 0.4μM, and [L] = 56μM (total lipid corrected for exterior lipid). This data was best fit with a cooperativity factor (σ) of 12. This indicates that the third cation binding site, present only with lipid, has higher affinity than the first two sites by a factor of 12. To illustrate the difference in affinity, this data was overlayed with the Tb^{3+} binding isotherm in the absence of lipid (black circles). The slight increase in cation binding affinity in the presence of lipid suggests that the cation and lipid binding sites are weakly linked.

To test the observation of a weak linkage between the cation and lipid binding sites in the shortened construct, Ca^{2+} was then titrated into a solution of C2A and sub-saturating concentrations of a membrane incorporated probe, Dansyl DHPE (50:40:10

POPC:POPS:Dansyl DHPE) (Figure 17). In this titration, there will not be an increase in FRET unless the addition of cation increases the affinity of the construct for lipid, i.e. linkage. The presence of some FRET is consistent with weak linkage. The resulting isotherm was analyzed with Equation 3, while holding all values except the cation binding affinity constant. It was calculated that the Ca^{2+} binding constant is K= $2.00x10^4$ M^{-1}, corresponding to -5.8 kcal/mol. This corresponds to a difference of 0.5 kcal/mol between the Ca^{2+} and Tb^{3+} associated binding constants and under conditions where both cation and lipid are present, Tb^{3+} is a mimic for Ca^{2+}.

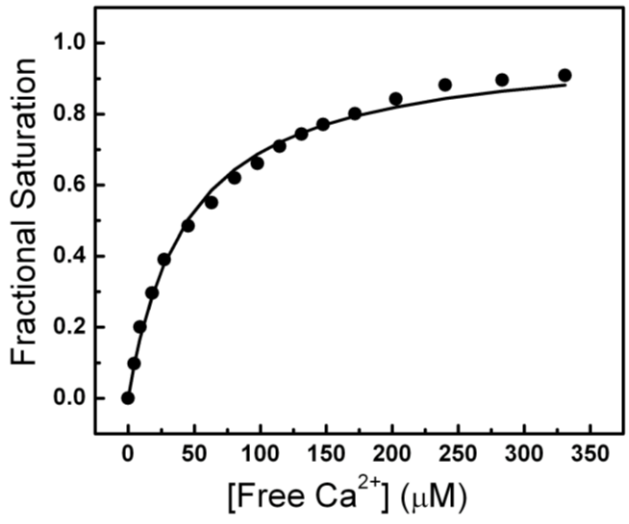

Figure 17

Short C2A titration with Ca^{2+} in the presence of 50 μM of a membrane incorporated probe, Dansyl DHPE (50:40:10 POPC:POPS:Dansyl DHPE). The signal arises from the quenching of the intrinsic protein fluorescence by the Dansyl DHPE probe. The lipid affinity of C2A increases as Ca^{2+} is titrated into solution. This is consistent with the cation and lipid sites being weakly linked under these titration conditions.

4.2.4 Ca^{2+} Binding: Isothermal Titration Calorimetry of short and long C2A

To further test the validity of Tb^{3+} as a Ca^{2+} mimic and to directly measure cation binding by the short C2A construct, ITC was carried out (Figure 18). 15 mM Ca^{2+} was titrated into solutions of 503 μM and 408 μM short C2A in the absence of lipid. Fitting the data with the Wiseman isotherm (*62*) resulted in a dissociation constant of (K_d) = $8.3x10^{-4}$ M^{-1}, ΔH= 3.55 kcal/mol, ΔG= -4.10 kcal/mol, and TΔS= 7.65 kcal/mol. The binding affinity (K_d), the enthalpy change upon binding (ΔH), and the number of cation binding sites (n) are fitting parameters in the Wiseman isotherm. This data was best fit with n= 0.80. It has been previously shown that C2A binds two cations in the absence of acidic lipids (18). Using this information, the data was also fit by fixing n = 2.0 and allowing the remaining two parameters to float (data not shown). This reduces the number of free variables while fitting the data. The result corresponds to a negligible change in free energy (0.37 kcal/mol) compared to n= 0.80. 15 mM Ca^{2+} was also titrated into a solution containing 450 μM long C2A in the absence of lipid (Figure 19). This data was best fit with a three site sequential model with dissociation constants of (K_d) = $1.9x10^{-4}$, $1.4x10^{-3}$, and $5.0x10^{-3}$ M^{-1}, ΔH = 2.43, 2.77, and -3.27 kcal/mol, ΔG = -4.85, -3.80, -3.27 kcal/mol, and TΔS = 7.28, 7.63, -0.2 kcal/mol. Neither the Wiseman isotherm nor a cooperative model fit the long C2A ITC data (data not shown), whereas the short C2A ITC data did not fit a sequential or cooperative model.

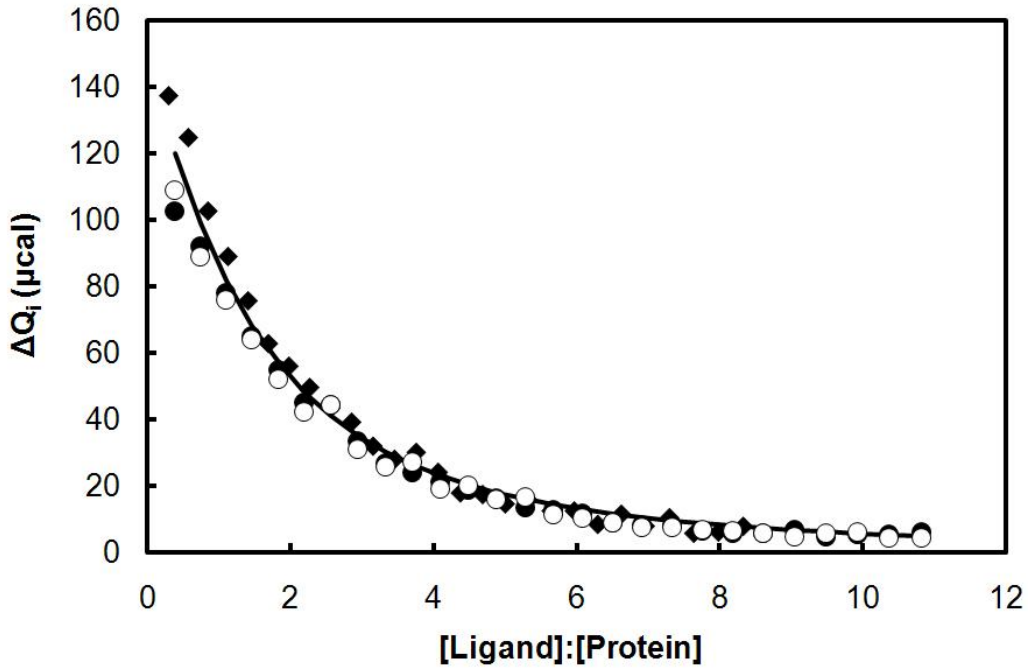

Figure 18

ITC results of short C2A Ca^{2+} titration in the absence of lipid. 15 mM Ca^{2+} was titrated into solutions of 503 µM C2A (black diamonds) and 408 µM C2A (black and open circles). Globally fitting the data with the Wiseman isotherm resulted in dissociation constant (K_d) of $8.3x10^{-4}$ M^{-1}, ΔH= 3.5 kcal/mol, ΔG = -4.10 kcal/mol, $T\Delta S$ = 7.65 kcal/mol and was best fit with n=0.80. The heat of dilution has been subtracted.

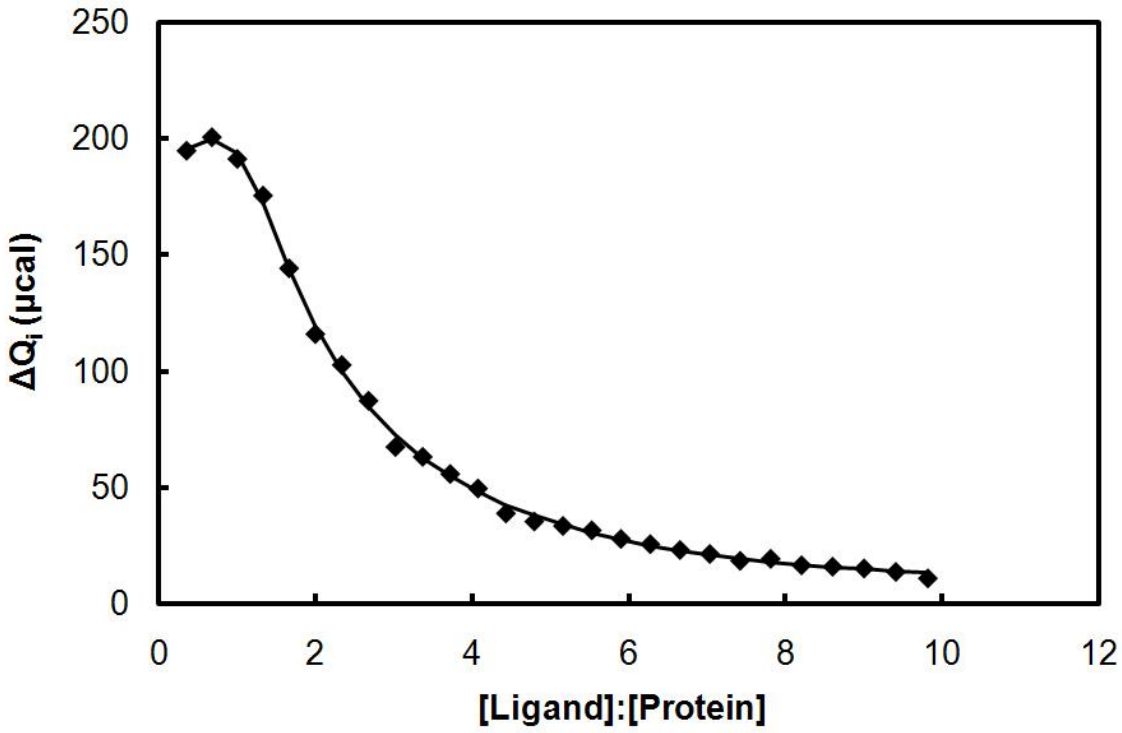

Figure 19

ITC results of long C2A Ca^{2+} titration in the absence of lipid. 15 mM Ca^{2+} was titrated into a solution of 450 μM long C2A (black diamonds) and was best fit with a three site sequential model resulting in (K_d) = $1.9x10^{-4}$, $1.4x10^{-3}$, and $5.0x10^{-3}$ M^{-1}, ΔH = 2.43, 2.77, and -3.27 kcal/mol, ΔG = -4.85, -3.80, -3.27 kcal/mol, and TΔS = 7.28, 7.63, -0.2 kcal/mol.

4.3.0 THERMODYNAMIC CYCLE

Considering this weak linkage relationship between the cation and lipid binding sites, we propose the thermodynamic cycle shown in Figure 20 to explain the binding behavior of the short C2A construct. The light gray portion of the figure ([PXXX] state where P is C2A and X is cation) was excluded in the derivations of all the partition functions described, as this state has a negligibly low probability of occurring. To test this

model, Equation 4 was derived to fit the cation binding data shown in Figure 16. To fit the cation binding data in the presence of lipid, a cooperativity factor (σ) of 12 was necessary, as in the presence of lipid the shortened construct has a third site that has a higher affinity for cation than the other two cation sites. This means that in the presence of lipid, the probability of the third cation site being occupied is 12 times greater than the probability of the first 2 sites being occupied. This may be contrasted to the scenario in the absence of lipid where the third site has an extremely low probability of being occupied, yet the first two sites have a reasonable probability of being occupied by cation. In the presence of lipid, the cation concentration of 50% occupancy of the third site is represented by its K_D ($1/\sigma K_A$) of 1.7 μM while the first two sites are 50% occupied at a cation concentration of 20 μM which is the same in the presence and absence of lipid.

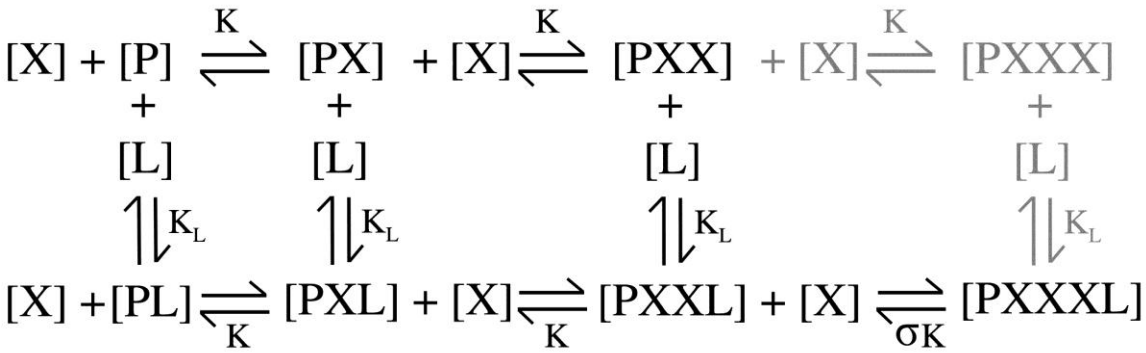

Figure 20

Proposed thermodynamic cycle for Syt1 C2A shortened construct binding, where [X] = cation, [P] = C2A, K = cation binding affinity ($K= 5x10^4\ M^{-1}$), K_L = lipid binding affinity ($3.3x10^5\ M^{-1}$), and σ = the cooperativity factor. The [PXXX] term (shown in light gray) is excluded from the thermodynamic cycle above because the extremely low probability of that state existing in the absence of lipid.

4.4.0 DISCUSSION

There is evidence in the literature for cation binding by the short C2A construct to be best described by a sequential model as opposed to an allosteric transition model. The sequential model was elucidated by NMR as directly identified by the occurrence of cross peaks upon Ca^{2+} ligation (*19*). In a sequential binding model, all three cation binding sites are present in the absence of acidic phospholipid. The three sites act independently and become occupied in a defined order from highest to lowest affinity. To directly investigate the differences in binding behavior between the long and short construct, we carried out a binding partition function analysis on the short C2A construct. Our data was fit using an allosteric transition model and was also tested against a sequential model as a control. It is important to note that both models fit our data well. The allosteric transition model is a better representation of our data because adding the additional parameter necessary for the sequential model does not yield a better fit (data not shown). Therefore, in this context, we cannot justify using the more complex sequential model.

We found that the short construct of C2A differs from the long construct in its overall diminished cooperativity between binding sites. As a consequence of reduced cooperativity, the short construct does not exhibit a linkage between the two cation binding sites present in the absence of lipid. The strictly hyperbolic binding isotherm (Figure 14A, Figure 18) is indicative of independent site binding. Through partition function analysis, the first two cation binding sites are shown to bind with equal affinity. Both sites have equal probability of cation occupation. This is in direct contrast with the

long construct that has been shown to bind cations in a cooperative manner (Figure 14B). The weakly sigmoidal shape of the binding isotherm of the long construct indicates the magnitude of cooperativity between the sites, even the absence of acidic phospholipids.

It is possible that this difference is caused by inadequate formation of the short construct's binding sites. A two site, equal affinity and one site binding partition function simplify to the same equation (Eq. 2), making it very difficult to differentiate the difference between the two systems. However, two sites of differing affinity of greater than 10X would be possible to differentiate and does not correspond to the data. To measure the number of cation binding sites in the presence lipid, a stoichiometry analysis was conducted. The Tb^{3+} titration was carried out under conditions of extreme excess of phospholipids, causing the protein to bind Tb^{3+} irreversibly. The excess phospholipid drives the protein toward being fully saturated with cation. Analysis of this irreversible binding isotherm shows three intact cation binding sites. An ITC experiment was also done to verify that two cation binding sites exist in the absence of lipid (Figure 18).

To enable a binding partition function analysis, the system was rigorously controlled and titrations were carried out in a specific order of increasing complexity. Independent binding isotherms are difficult to accurately fit if more than one binding association constant is involved as a fitting parameter. To circumvent this problem, each isotherm was fit using only one free variable in the partition function while holding all previously determined association constants fixed. In this way, the only free variable while fitting the most complex system (cation binding the presence of acidic phospholipids) is the cooperativity factor (σ).

To directly measure the lipid binding affinity (K_L) using fluorescence spectroscopy, a suspension of dansylated lipids, (50:40:10 POPC:POPS:Dansyl DHPE) LUV, were titrated into solution containing C2A short in the absence of cation. The loss of protein fluorescence was due to FRET associated with membrane, specifically the dansyl probe, binding. To evaluate the linkage between phospholipid and cation binding sites, the titration was repeated in the presence of increasing concentrations of Ca^{2+}. Since Ca^{2+} does not cause FRET upon ligation with protein, the change in fluorescence intensity was only caused by liposome binding. Surprisingly, there was very little influence of physiological levels of Ca^{2+} on lipid binding affinity of C2A short. The resulting binding isotherms (Figure 15 left panel) were fit using Equation 3. The negligible change in lipid binding affinity induced by cation presence is indicative of a lack of cooperativity between binding sites.

The binding affinity of the third cation binding site was measured by titrating Tb^{3+} into short C2A in the presence of sub-saturating lipids. The small shift in the resulting binding isotherm indicates a slightly higher affinity for cation in the presence of lipid (Figure 16). The cooperativity in the third site could be determined, as the cooperativity factor (σ) was the only free parameter. Our analysis has shown the presence of acidic phospholipid induces the formation of a third cation binding site in C2A short that has higher affinity than the two, solution state binding sites consistent with the original suggestion of Rizo (*19*).

The validity of Tb^{3+} as a Ca^{2+} mimic could be evaluated by the use of fluorescence spectroscopy and ITC experiments. Using fluorescence spectroscopy, both

cations, Tb^{3+} and Ca^{2+}, were found to bind with similar affinity (difference of 0.5 kcal/mol) in the presence of lipid (Figures 16 and 17). However, in the solution state, when the fluorescence and ITC results are compared, we find that there is a free energy difference of 2.15 kcal/mol per solution state cation site. Different cations were used in the fluorescence and calorimetry experiments and, because the fluorescence data is consistent with both cations in the presence of membrane, the differences may be magnified in solution. Calorimetry required ~1000X the protein concentration to generate enough heat to produce a useable binding isotherm in comparison to the protein concentration necessary for a robust fluorescence spectroscopy signal. The weak signal in ITC is due to the very low enthalpy associated with this protein-cation association as it is an entropy dominated binding process. This may reduce the sensitivity of the measurement, although both fluorescence and ITC results are consistent with an independent site binding model.

Recently, the cation–protein interaction of the long construct Syt1 C2A (97-273) was tested by ITC (*63*). Their findings concluded that the binding could not be characterized by the independent model and rather was best fit by the sequential binding model, even though similar experimental conditions to those presented here were utilized (*63*). The long and short ITC binding data were different in that the first few injection points of the long data had an increasing heat produced whereas the short data is characterized by a gradually decreasing endotherm (Figures 18 and 19).

To model the binding behavior of the short C2A construct, a thermodynamic cycle consistent with all of the binding data was constructed (Figure 20). In this model,

the presence of lipid increases the probability of a third cation being bound. This is consistent with the allosteric transition model proposed for the long construct. However, there are drastic differences between the constructs in the impact of lipid binding on the cooperativity on ligation of a third cation as well as the lack of weak cooperativity between the first two cation sites as was observed in the long construct. Overall, we find a reduction in communication between binding sites of the short construct when compared to the long construct. These results suggest that the use of specific C2A constructs to study Syt1 function must be selected with care. In terms of physiological function, we find a difference in how binding information is disseminated through the constructs as manifested in the extent of linkage between binding sites as well as the magnitude (or lack thereof) of cooperativity. This suggests that the C2 domain is a transducer of cation occupancy signals and sensitive to its environment by the residues of this motif being intimately coupled together.

REFERENCES

1. Hui, E. F., Bai, J. H., Wang, P., Sugimori, M., Llinas, R. R., and Chapman, E. R. (2005) Three distinct kinetic groupings of the synaptotagmin family: Candidate sensors for rapid and delayed exocytosis, *Proceedings of the National Academy of Sciences of the United States of America 102*, 5210-5214.
2. Südhof, T. C. (2002) Synaptotagmins: Why So Many?, *Journal of Biological Chemistry 277*, 7629-7632.
3. Bhalla, A., Chicka, M. C., Tucker, W. C., and Chapman, E. R. (2006) Ca^{2+}-synaptotagmin directly regulates t-SNARE function during reconstituted membrane fusion, *Nature Structural & Molecular Biology 13*, 323-330.
4. Dennison, S. M., Bowen, M. E., Brunger, A. T., and Lentz, B. R. (2006) Neuronal SNAREs do not trigger fusion between synthetic membranes but do promote PEG-mediated membrane fusion, *Biophysical Journal 90*, 1661-1675.
5. C. G., Eng, W. S., Melia, T. J., and Rothman, J. E. (2006) A clamping mechanism involved in SNARE-dependent exocytosis, *Science 313*, 676-680.
6. Lu, X. B., Xu, Y. B., Zhang, F., and Shin, Y. K. (2006) Synaptotagmin I and Ca^{2+} promote half fusion more than full fusion in SNARE-mediated bilayer fusion, *FEBS Letters 580*, 2238-2246.
7. Rickman, C., Jimenez, J. L., Graham, M. E., Archer, D. A., Soloviev, M., Burgoyne, R. D., and Davletov, B. (2006) Conserved prefusion protein assembly in regulated exocytosis, *Molecular Biology of the Cell 17*, 283-294.
8. Dai, H., Shen, N., Araç, D., and Rizo, J. (2007) A quaternary SNARE-synaptotagmin-Ca^{2+}-phospholipid complex in neurotransmitter release, *Journal of Molecular Biology 367*, 848-863.
9. Martens, S., Kozlov, M. M., and McMahon, H. T. (2007) How synaptotagmin promotes membrane fusion, *Science 316*, 1205-1208.
10. Chen, X. C., Araç, D., Wang, T. M., Gilpin, C. J., Zimmerberg, J., and Rizo, J. (2006) SNARE-mediated lipid mixing depends on the physical state of the vesicles, *Biophysical Journal 90*, 2062-2074.
11. Davletov, B. A., and Südhof, T. C. (1993) A single C2 domain from synaptotagmin I is sufficient for high affinity Ca^{2+}/phospholipid binding, *Journal of Biological Chemistry 268*, 26386-26390.
12. Sutton, R. B., Davletov, B. A., Berghuis, A. M., Südhof, T. C., and Sprang, S. R. (1995) Structure of the first C2 domain of synaptotagmin I: a novel Ca^{2+}/phospholipid-binding fold, *Cell 80*, 929-938.
13. Chapman, E. R., and Jahn, R. (1994) Calcium-dependent interaction of the cytoplasmic region of the synaptotagmin with membranes - Autonomous function of a single C2 homologous domain, *Journal of Biological Chemistry 269*, 5735-5741.
14. Südhof, T. C., and Rizo, J. (1996) Synaptotagmins: C-2-domain proteins that regulate membrane traffic, *Neuron 17*, 379-388.
15. Shao, X. G., Fernandez, I., Zhang, X. Y., Südhof, T. C., and Rizo, J. (1997) Synaptotagmin-syntaxin interaction: The C-2 domain as a Ca^{2+}-dependent electrostatic switch, *Neuron 18*, 133-142.

16. Chapman, E. R., and Davis, A. F. (1998) Direct Interaction of a Ca^{2+}-binding Loop of Synaptotagmin with Lipid Bilayers, *Journal of Biological Chemistry 273*, 13995-14001.
17. Thomas, D. M., and Elferink, L. A. (1998) Functional analysis of the C2A domain of synaptotagmin 1: Implications for calcium-regulated secretion, *Journal of Neuroscience 18*, 3511-3520.
18. Zhang, X. Y., Rizo, J., and Südhof, T. C. (1998) Mechanism of phospholipid binding by the C2A-domain of synaptotagmin I, *Biochemistry 37*, 12395-12403.
19. Davis, A. F., Bai, J. H., Fasshauer, D., Wolowick, M. J., Lewis, J. L., and Chapman, E. R. (1999) Kinetics of synaptotagmin responses to Ca^{2+} and assembly with the core SNARE complex onto membranes, *Neuron 24*, 363-376.
20. Bai, J. H., Earles, C. A., Lewis, J. L., and Chapman, E. R. (2000) Membrane-embedded synaptotagmin penetrates cis or trans target membranes and clusters via a novel mechanism, *Journal of Biological Chemistry 275*, 25427-25435.
21. Fukuda, M., and Mikoshiba, K. (2000) Distinct self-oligomerization activities of synaptotagmin family - Unique calcium-dependent oligomerization properties of synaptotagmin VII, *Journal of Biological Chemistry 275*, 28180-28185.
22. Garcia, R. A., Forde, C. E., and Godwin, H. A. (2000) Calcium triggers an intramolecular association of the C2 domains in synaptotagmin, *Proceedings of the National Academy of Sciences of the United States of America 97*, 5883-5888.
23. Fernández-Chacón, R., Konigstorfer, A., Gerber, S. H., Garcia, J., Matos, M. F., Stevens, C. F., Brose, N., Rizo, J., Rosenmund, C., and Südhof, T. C. (2001) Synaptotagmin I functions as a calcium regulator of release probability, *Nature 410*, 41-49.
24. Fukuda, M., Kanno, E., Ogata, Y., and Mikoshiba, K. (2001) Mechanism of the SDS-resistant synaptotagmin clustering mediated by the cysteine cluster at the interface between the transmembrane and spacer domains, *Journal of Biological Chemistry 276*, 40319-40325.
25. Ubach, J., Lao, Y., Fernandez, I., Araç, D., Südhof, T. C., and Rizo, J. (2001) The C2B domain of synaptotagmin I is a Ca^{2+}-binding module, *Biochemistry 40*, 5854-5860.
26. Bai, J. H., Wang, P., and Chapman, E. R. (2002) C2A activates a cryptic Ca^{2+}-triggered membrane penetration activity within the C2B domain of synaptotagmin I, *Proceedings of the National Academy of Sciences of the United States of America 99*, 1665-1670.
27. Fernández-Chacón, R., Shin, O. H., Konigstorfer, A., Matos, M. F., Meyer, A. C., Garcia, J., Gerber, S. H., Rizo, J., Südhof, T. C., and Rosenmund, C. (2002) Structure/function analysis of Ca^{2+} binding to the C2A domain of synaptotagmin 1, *Journal of Neuroscience 22*, 8438-8446.
28. Wu, Y., He, Y. H., Bai, J. H., Ji, S. R., Tucker, W. C., Chapman, E. R., and Sui, S. F. (2003) Visualization of synaptotagmin I oligomers assembled onto lipid monolayers, *Proceedings of the National Academy of Sciences of the United States of America 100*, 2082-2087.

29. Yoshihara, M., Adolfsen, B., and Littleton, J. T. (2003) Is synaptotagmin the calcium sensor?, *Current Opinion in Neurobiology 13*, 315-323.
30. Bai, J. H., and Chapman, E. R. (2004) The C2 domains of synaptotagmin - partners in exocytosis, *Trends in Biochemical Sciences 29*, 143-151.
31. Rhee, J. S., Li, L. Y., Shin, O. H., Rah, J. C., Rizo, J., Südhof, T. C., and Rosenmund, C. (2005) Augmenting neurotransmitter release by enhancing the apparent Ca^{2+} affinity of synaptotagmin 1, *Proceedings of the National Academy of Sciences of the United States of America 102*, 18664-18669.
32. Araç, D., Chen, X. C., Khant, H. A., Ubach, J., Ludtke, S. J., Kikkawa, M., Johnson, A. E., Chiu, W., Südhof, T. C., and Rizo, J. (2006) Close membrane-membrane proximity induced by Ca^{2+}-dependent multivalent binding of synaptotagmin-1 to phospholipids, *Nature Structural & Molecular Biology 13*, 209-217.
33. Rizo, J., Chen, X. C., and Araç, D. (2006) Unraveling the mechanisms of synaptotagmin and SNARE function in neurotransmitter release, *Trends in Cell Biology 16*, 339-350.
34. Takamori, S., Holt, M., Stenius, K., Lemke, E. A., Gronborg, M., Riedel, D., Urlaub, H., Schenck, S., Brugger, B., Ringler, P., Muller, S. A., Rammner, B., Grater, F., Hub, J. S., De Groot, B. L., Mieskes, G., Moriyama, Y., Klingauf, J., Grubmuller, H., Heuser, J., Wieland, F., and Jahn, R. (2006) Molecular anatomy of a trafficking organelle, *Cell 127*, 831-846.
35. Tang, J., Maximov, A., Shin, O. H., Dai, H., Rizo, J., and Südhof, T. C. (2006) A complexin/synaptotagmin 1 switch controls fast synaptic vesicle exocytosis, *Cell 126*, 1175-1187.
36. Zimmerberg, J., Akimov, S. A., and Frolov, V. (2006) Synaptotagmin: fusogenic role for calcium sensor?, *Nature Structural & Molecular Biology 13*, 301-303.
37. Stein, A., Radhakrishnan, A., Riedel, D., Fasshauer, D., and Jahn, R. (2007) Synaptotagmin activates membrane fusion through a Ca^{2+}-dependent trans interaction with phospholipids, *Nature Structural & Molecular Biology 14*, 904-911.
38. Chapman, E. R. (2008) How does synaptotagmin trigger neurotransmitter release?, *Annual Review of Biochemistry 77*, 615-641.
39. Chicka, M. C., Hui, E. F., Liu, H. S., and Chapman, E. R. (2008) Synaptotagmin arrests the SNARE complex before triggering fast, efficient membrane fusion in response to Ca^{2+}, *Nature Structural & Molecular Biology 15*, 827-835.
40. Lingwood, D., Ries, J., Schwille, P., and Simons, K. (2008) Plasma membranes are poised for activation of raft phase coalescence at physiological temperature, *Proceedings of the National Academy of Sciences of the United States of America 105*, 10005-10010.
41. Rizo, J., and Rosenmund, C. (2008) Synaptic vesicle fusion, *Nature Structural & Molecular Biology 15*, 665-674.
42. Shahin, V., Datta, D., Hui, E., Henderson, R. M., Chapman, E. R., and Edwardson, J. M. (2008) Synaptotagmin perturbs the structure of phospholipid bilayers, *Biochemistry 47*, 2143-2152.

43. Wickner, W., and Schekman, R. (2008) Membrane fusion, *Nature Structural & Molecular Biology 15*, 658-664.
44. Li, L. Y., Shin, O. H., Rhee, J. S., Araç, D., Rah, J. C., Rizo, J., Südhof, T., and Rosenmund, C. (2006) Phosphatidylinositol phosphates as co-activators of Ca^{2+} binding to C2 domains of synaptotagmin 1, *Journal of Biological Chemistry 281*, 15845-15852.
45. Hui, E. F., Bai, J. H., and Chapman, E. R. (2006) Ca^{2+}-triggered simultaneous membrane penetration of the tandem C2-domains of synaptotagmin I, *Biophysical Journal 91*, 1767-1777.
46. Jackson, M. B., and Chapman, E. R. (2008) The fusion pores of Ca^{2+}-triggered exocytosis, *Nature Structural & Molecular Biology 15*, 684-689.
47. Shin, O. H., Rhee, J. S., Tang, J., Sugita, S., Rosenmund, C., and Südhof, T. C. (2003) Sr^{2+} binding to the Ca^{2+} binding site of the synaptotagmin 1 C2B domain triggers fast exocytosis without stimulating SNARE interactions, *Neuron 37*, 99-108.
48. Sørensen, J. B. (2004) Formation, stabilisation and fusion of the readily releasable pool of secretory vesicles, *Pflugers Archiv-European Journal of Physiology 448*, 347-362.
49. Sorensen, J. B., Nagy, G., Varoqueaux, F., Nehring, R. B., Brose, N., Wilson, M. C., and Neher, E. (2003) Differential control of the releasable vesicle pools by SNAP-25 splice variants and SNAP-23, *Cell 114*, 75-86.
50. Nalefski, E. A., Wisner, M. A., Chen, J. Z., and Sprang, S. R. (2001) C2 domains from different C^{a2+} signaling pathways display functional and mechanistic diversity, *Biochemistry 40*, 3089-3100.
51. Frazier, A. A., Roller, C. R., Havelka, J. J., Hinderliter, A., and Cafiso, D. S. (2003) Membrane-bound orientation and position of the synaptotagmin I C2A domain by site-directed spin labeling, *Biochemistry 42*, 96-105.
52. Fernandez, I., Araç, D., Ubach, J., Gerber, S. H., Shin, O. H., Gao, Y., Anderson, R. G. W., Südhof, T. C., and Rizo, J. (2001) Three-dimensional structure of the synaptotagmin 1 C2B-domain: Synaptotagmin 1 as a phospholipid binding machine, *Neuron 32*, 1057-1069.
53. Hilser, V. J., and Thompson, E. B. (2007) Intrinsic disorder as a mechanism to optimize allosteric coupling in proteins, *Proceedings of the National Academy of Sciences of the United States of America 104*, 8311-8315.
54. Kertz, J. A., Almeida, P. F. F., Frazier, A. A., Berg, A. K., and Hinderliter, A. (2007) The cooperative response of synaptotagmin IC2A. A hypothesis for a Ca^{2+}-driven molecular hammer, *Biophysical Journal 92*, 1409-1418.
55. Damer, C. K., and Creutz, C. E. (1994) Synergistic membrane interactions of the 2 C2 domains of synaptotagmin, *Journal of Biological Chemistry 269*, 31115-31123.
56. Guan, K. L., and Dixon, J. E. (1991) Eukaryotic proteins expressed in Escherichia coli: an improved thrombin cleavage and purification procedure of fusion proteins with glutathione S-transferase, *Analytical Biochemistry 192*, 262-267.

57. Wang, C. T., Grishanin, R., Earles, C. A., Chang, P. Y., Martin, T. F. J., Chapman, E. R., and Jackson, M. B. (2001) Synaptotagmin modulation of fusion pore kinetics in regulated exocytosis of dense-core vesicles, *Science 294*, 1111-1115.
58. Wang, C. T., Bai, J. H., Chang, P. Y., Chapman, E. R., and Jackson, M. B. (2006) Synaptotagmin-Ca^{2+} triggers two sequential steps in regulated exocytosis in rat PC12 cells: fusion pore opening and fusion pore dilation, *Journal of Physiology-London 570*, 295-307.
59. Simons , K., and van Meer, G. (1988). Lipid sorting in epithelial cells. *Biochemistry* **17**, 6197-6202.
60. Field, K.A, Holowka, D., Baird, B. (1997). Compartmentalized activation of the high affinity immunoglobulin E receptor within membrane domains. *J Biol Chem.* **272,** 4276-4280.
61. Sheets, E.D., Holowka, D., and Baird B. (1999). Membrane organization in immunoglobulin E receptor signaling. *Curr Opin Chem Biol.* **3,** 95-99.
62. Bernardino de la Serna, J., Perez-Gil, J., Simonsen, A.C., Bagatolli, L.A. (2004). Cholesterol rules: Direct observation of the coexistence of two fluid phases in native pulmonary surfactant membranes at physiological temperatures. *J Biol Chem.* **279,** 40715-40722.
63. Rogasevskaia, T., Coorssen, J.R. (2006). Sphingomyelin-enriched microdomains define the efficiency of native Ca^{2+} -triggered membrane fusion. *J Cell Sci*. **119,** 2688-2694.
64. Baumgart , T., Hunt, G., Farkas, E.R., Webb, W.W., and Feigenson, G.W. (2007). Fluorescence probe partitioning between L_o/L_d phases in lipid membranes. *Biochim Biophys Acta*. **1768,** 2182-2194.
65. Thompson, T.E. and Tillack, T.W. (1985). Organization of Glycosphingolipids in Bilayers and Plasma Membranes of Mammalian Cells. *Annu Rev Biophys Biophys Chem*. **14,** 361-386.
66. Simons, K. and Ikonen, E. (1997). Functional rafts in cell membranes. *Nature* **387,** 569-572.
67. Brown, D.A, London, E. (2000). Structure and Function of Sphingolipid-and Cholesterol- Rich Membrane Rafts. *J Biol Chem*. **275,** 17221-17224.
68. McConnell, H.M. and Vrljic, M. (2003). Liquid-Liquid Immiscibility in Membranes. *Annu Rev Biophys Biomol Struct*. **32**, 469-492.
69. Edidin, M. (2003). The State of Lipid Rafts: From Model Membranes to Cells. *Annu Rev Biophys Biomol Struct.* **32,** 257-283.
70. Simons, K., Vaz, W.L. (2004). Model Systems, Lipid Rafts, and Cell Membranes. *Annu Rev Biophys Biomol Struct.* **33,** 269-295.
71. Suurkuusk, J., Lentz, B.R., Barenholz, Y., Biltonen, R.L., and Thomson, T.E. (1976). A calorimetric and fluorescent probe study of the gel-liquid crystalline phase transition in small, single-lamellar dipalmitoylphosphatidylcholine vesicles. *Biochemistry **15***, 1393-401.
72. Mountcastle, D.B., Biltonen, R.L., and Halsey, M.J. (1978). Effect of anesthetics and pressure on the thermotropic behavior of multilamellar.

73. Silvius, J.R., Gagné, J. (1984). Calcium-Induced fusion of lateral phase separations in phosphatidylcholine-phosphatidylserine vesicles. Correlation by calometric and fusion measurements. *Biochemistry* **23,** 3232-3240.
74. Ipsen, J.H., Karlström, G., Mouritsen, O.G., Wennerström, H., and Zuckermann, M.J. (1987). Phase equilibria in the phosphatidylcholine-cholesterol system. *Biochim. Biophys. Acta* **1**, 162-72.
75. Sankaram, M.B., and Thompson, T.E. (1990). Modulation of phospholipid acyl chain order by cholesterol. A solid state ^{2}H Nuclear Magnetic Resonance Study. *Biochemistry* **29,** 10676-10684.
76. Heimburg, T., Würz, U., Marsh, D. (1992). Binary phase diagram of hydrated dimyristoylglycerol-dimyristoylphosphatidylcholine mixtures. *Biophys J.* **63**, 1369-1378.
77. Bloom, M., Thewalt, J.L. (1995). Time and distance scales of membrane domain organization. *Mol Membr Biol.* **12,** 9-13.
78. Mendelsohn, R., Liang, G.L., Strauss, H.L., Snyder, R.G. (1995). IR spectroscopic determination of gel state miscibility in long-chain phosphatidyl choline mixtures. *Biophys J.* **69,** 1987-1998.
79. Garidel, P., Johann, C., Blume, A. (1997). Nonideal mixing and phase separation in phosphatidylcholine-phosphatidic acid mixtures as a function of acyl chain length and pH. *Biophys J.* **72,** 2196-2210.
80. Keller, S.L., McConnell, H.M. (1999). Stripe Phases in Lipid Monolayers near a miscibility Critical Point. *Phys Rev Lett.* **82**, 1602-1605.
81. Huang, J., Feigenson, G. (1999). A Microscopic Interaction Model of Maximum solubility of Cholesterol in Lipid Bilayers. *Biophys J.* **4**, 2142-2157.
82. Radhakrishnan, A., McConnell, H.M. (1999). Condensed Complexes of Cholesterol and Phospholipids. *Biophys J.* **77**, 1507-1517.
83. Cao, H., Zhang, J., Jing, B., Regen, S.L. (2005). A Chemical Sensor for the Liquid-Ordered Phase. *J Am Chem Soc.* **127**, 8813-8816.
84. Kinnunen, P. K. J. (1991). On the principles of functional ordering in biological membranes. *Chem. Phys. Lipids.* **57,** 375-399.
85. Thompson, T. E., M. B. Sankaram, and R. L. Biltonen. (1992). Biological membrane domains: functional significance. Comments Mol. Cell. Biophys. **8,** 1-15.
86. Thompson, T.E., Sankaram, M.B., Biltonen, R.L., Marsh, D., Vaz W.L.C. (1995). Effects of domain structure of in-plane reactions and interactions. *Mol Membr Biol.* **12,** 157-162.
87. Melo, E. C. C., Lourtie, I. M. G., Sankaram, M. B., Thompson, T. E., and Vaz, W.L. C. (1992). Effects of domain connection and disconnection on the yields of in-plane bimolecular reaction in membranes. *Biophys. J.* **63,** 1506 -1512.
88. Majumder R, Quinn-Allen MA, Kane WH, Lentz BR. (2005). The Phosphatidylserine Binding Site of the Factor V(a) C2 Domain Accounts for Membrane Binding but Does Not Contribute to the Assembly or Activity of a Human Factor X(a)-Factor V(a) Complex. *Biochemistry* **44,** 711-8.

89. White, S. H., Wimley, W. C., Ladokhin, A. S., and Hristova, K. (1998). Protein folding in membranes: Determining energetics of peptide-bilayer interactions. *Meth Enzym.* **295,** 62-87.
90. Kim, J., Mosior, M., Chung, L.A., Wu, H. McLaughlin, S. (1991). Binding of peptides with basic residues to membranes containing acidic phospholipids. *Biophys J.* **60**, 135-148.
91. Almeida, P. F. F., Pokorny, A., and Hinderliter, A. (2005). Thermodynamics of membrane domains. *Biochim. Biophys. Acta* **1720**, 1-13.
92. Almeida, P.F.F. (2009). Thermodynamics of lipid interactions in complex bilayers. *Biochim Biophys Acta* **1788,** 72-85.
93. Ladokhin, A. S., Jayasinghe, S. and White, S. H. (2000). How to measure and analyze tryptophan fluorescence in membranes propertly, and why bother? *Anal Biochem* **285**, 235-245.
94. Freire. E, Mayorga, O. and Straume, M. (1990). Isothermal Titration Calorimetry. *Analytical Chemistry*, **62**, 950A-959A.
95. Seelig, J. (1997). Titration calorimetry of lipid-peptide interactions. *Biochimica et Biophysica Acta* **1331**, 103-116.
96. Wyman J., and Gill, S.J, "Binding and Linkage," University Science Books, Mill Valley, CA, 1990.
97. Dill, K.A., Bromberg, S. "Molecular Driving Forces." Garland Science, New York, NY 2002.
98. Almeida, P. F. F., Sohma, H., Rasch, K., Wieser, C. M., and Hinderliter, A. (2005). Allosterism in membrane binding: a common motif of the annexins? *Biochemistry* **44,** 10905-10913.
99. Hinderliter, A. K., Almeida, P. F. F., Creutz, C. E., and Biltonen, R. L. (2001). Domainformation in a fluid mixed bilayer modulated through binding of the C2 protein motif. *Biochemistry* **40**, 4181-4191.
100. Hinderliter, A., Biltonen, R. L., and Almeida, P. F. F. (2004). Lipid modulation of protein induced membrane domains as a mechanism for controlling signal transduction. *Biochemistry* **43,** 7102-7110.
101. Wiseman, T., Williston, S., Brandts, J. F., and Lin, L. N. (1989) Rapid measurement of binding constants and heats of binding using a new titration calorimeter, *Analytical Biochemistry 179*, 131-137.
102. Radhakrishnan, A., Stein, A., Jahn, R., and Fasshauer, D. (2009) The Ca^{2+} Affinity of Synaptotagmin 1 Is Markedly Increased by a Specific Interaction of Its C2B Domain with Phosphatidylinositol 4,5-Bisphosphate, *Journal of Biological Chemistry 284*, 25749-25760.